

**Suppression of pervasive noncoding transcription in embryonic stem cells by
esBAF**

Sarah J. Hainer^{1,2}, Weifeng Gu^{2,5}, Benjamin R. Carone^{3,6}, Benjamin D. Landry^{1,2}, Oliver
J. Rando³, Craig C. Mello^{2,4}, Thomas G. Fazzio^{1,2}

¹Department of Molecular, Cell, and Cancer Biology, University of Massachusetts
Medical School, Worcester, MA 01605, USA

²Program in Molecular Medicine, University of Massachusetts Medical School,
Worcester, MA 01605, USA

³Department of Biochemistry and Molecular Pharmacology, University of Massachusetts
Medical School, Worcester, MA 01605, USA

⁴Howard Hughes Medical Institute

⁵Current address: Department of Cell Biology and Neuroscience, University of California
at Riverside, Riverside, CA 92521, USA

⁶Current address: Biology Department, Williams College, Williamstown, MA 01267, USA

INVENTORY OF SUPPLEMENTAL MATERIAL

SUPPLEMENTAL MATERIALS AND METHODS

SUPPLEMENTAL FIGURE LEGENDS

SUPPLEMENTAL TABLE 1. Oligonucleotides used in this study.

SUPPLEMENTAL TABLE 2. Homology constructs used for creation of SB lines.

SUPPLEMENTAL FIGURE 1 accompanies Figures 1 and 2

SUPPLEMENTAL FIGURE 2 accompanies Figures 1 and 2

SUPPLEMENTAL FIGURE 3 accompanies Figures 1 and 2

SUPPLEMENTAL FIGURE 4 accompanies Figure 2

SUPPLEMENTAL FIGURE 5 accompanies Figure 2

SUPPLEMENTAL FIGURE 6 accompanies Figure 2

SUPPLEMENTAL FIGURE 7 accompanies Figure 2

SUPPLEMENTAL FIGURE 8 accompanies Figure 4

SUPPLEMENTAL FIGURE 9 accompanies Figures 3 and 4

SUPPLEMENTAL FIGURE 10 accompanies Figure 4

SUPPLEMENTAL FIGURE 11 accompanies Figure 5

SUPPLEMENTAL FIGURE 12 accompanies Figures 5 and 6

SUPPLEMENTAL FIGURE 13 accompanies Figure 7

SUPPLEMENTAL MATERIALS AND METHODS

Chromatin immunoprecipitation

Cells from RNAi-mediated KD in a 10 cm dish were crosslinked with a fixing solution (11% formaldehyde, 100 mM NaCl, 1 mM EDTA, 50 mM HEPES-KOH [pH 7.6]), incubated at room temperature for 10 min and quenched with glycine to a final concentration of 125 mM. Cells were washed with ice-cold PBS containing protease inhibitors (Thermo Scientific) and pelleted. Cell pellets were resuspended in 570 μ l SDS lysis buffer (1% SDS, 10 mM EDTA, 50 mM Tris [pH 8.0]) including protease inhibitors, incubated for 10 min on ice and sonicated in 15 ml conical tubes (BD Falcon) in a Bioruptor (UCD-200) at high, 2 times for 15 min of 30s on/30s off cycles followed by a 10,000 rcf spin at 4°C for 20 min. Supernatants were transferred to a new microfuge tube and pellets were discarded. 30 μ l of chromatin was stored overnight at 4°C for input samples while the remainder of the chromatin was diluted in 2.5 ml IP buffer (0.01% SDS, 1.1% TritonX-100, 1.2 mM EDTA, 16.7 mM Tris [pH 8.0], 167 mM NaCl), combined with antibody coupled magnetic beads, and incubated at 4°C overnight. H3 antibody (Abcam, ab1791), RNAPII (Santa Cruz, sc-9001), or IgG (Abcam, ab37415)

coupled protein A magnetic beads (NEB) were blocked with 5 mg/ml BSA overnight at 4°C. Magnetic beads were washed twice with IP buffer and 5 times with MVL buffer (50 mM Tris [pH 7.4], 250 mM NaCl, 1 mM EDTA, 0.1% TritonX-100) at 4°C for 5 min. Washed beads were eluted twice in 100 µl elution buffer (20 mM Tris [pH 8.0], 100 mM NaCl, 20 mM EDTA, 1% SDS), at 65°C on a thermomixer for 15 min. Eluted material was transferred to a new microfuge tube, combined and incubated at 65°C overnight to reverse crosslinking. Input DNA was diluted with 170 µl elution buffer and treated similarly. Samples were treated with RNaseA/T1 (Ambion) for 1 hr at 37°C and proteinase K (Ambion) for 1 hr at 55°C and then PCI extracted using phase-lock tubes (5 Prime). Ethanol precipitated ChIP-enriched DNA was then used as a template for quantitative PCR (qPCR) on an Eppendorf Realplex using a SYBR FAST kit (KAPA Biosystems) with specific primers (see primer table). Input DNA was used as a control for base-level enrichment and to calculate a standard curve. Occupancy was determined by the percent IP enrichment relative to input levels.

Micrococcal nuclease digestion

ES cells were crosslinked with formaldehyde (Sigma) to a final concentration of 1%, incubated at room temperature for 10 min and quenched with glycine to a final concentration of 125 mM. Cells were washed with ice cold PBS and pelleted. Cell pellets were resuspended in lysis buffer (10 mM Tris [pH 7.5], 10 mM NaCl, 2 mM MgCl₂, 0.5% NP-40, 1 mM CaCl₂) with protease inhibitors (Roche) and incubated for 15 min at 4°C. Permeabilized cells were treated with ~10 Units/10⁶ cells of micrococcal nuclease (Roche) for 5 min at 37°C. Reactions were stopped with the addition of EDTA. Control samples with no MNase addition were treated similarly. Samples were incubated for 4 hr at 4°C with rotation with RNaseA/T1 (Ambion) then incubated overnight at 65°C with 0.01% SDS and proteinase K (Ambion). DNA was extracted with PCI using phase-lock tubes, ethanol precipitated, and resuspended in 30 µL TE. Quality was confirmed through bioanalyzer analysis to ensure an equal size distribution of DNA fragments produced for each sample. For MNase-qPCR reactions, DNA was then used as a template for qPCR using a SYBR FAST kit (KAPA Biosystems) with specific primers (see primer table) on an Eppendorf Realplex. Undigested DNA was used as a control and to calculate a standard curve.

MNase-Seq

Library construction

Paired-end libraries of MNase digested DNA were prepared as described previously (Henikoff et al. 2011). Briefly, samples were treated with CIP, end-repaired, A-tailed, and adaptor-ligated as described (Illumina). Between each step, DNA was cleaned with PCI extraction and ethanol precipitation. After adaptor ligation, DNA was selected and purified with Agencourt Ampure beads and then PCR amplified with KAPA HiFi polymerase using 16 cycles of PCR. The library was then purified with a Qiagen PCR purification kit, its concentration determined using a NanoDrop (Thermo), and the integrity was confirmed by sequencing ~10 fragments from each library. Libraries were individually sequenced on an Illumina HiSeq2000 using paired-end sequencing (100 bp) at the UMass Medical School deep sequencing core facility.

Data analysis

Paired end reads were collapsed and adapter sequences were removed from fastq files. Reads were mapped to the mouse mm9 genome using Bowtie2 and only uniquely mapped reads with zero, one, or two mismatches were used for further analysis. The number of mapped reads for *EGFP* KD and for *Smarca4* KD MNase-Seq libraries is 231,336,591 and 225,479,272, respectively. The read size distribution was determined for each library and reads were sorted for nucleosome sized fragments (135-165). To calculate occupancy around TSS, DHS, or transcription factor sites, seqMINER (Ye et al. 2011) was used to sum read occurrence either 2000 bp upstream and downstream, 1000 bp upstream and downstream, or 500 bp upstream and downstream of the reference sequence. Occurrences were binned in 20 bp intervals and reads were normalized to the average genome-wide coverage. TSS reference sites were used based on mm9 TSS coordinates. DHS reference sites were based on mouse ENCODE data (GSM1014154). Coordinates of DHSs outside of TSSs were obtained by subtraction of called TSSs from ENCODE DHS coordinates (mm9).

CapSeq

Library construction

Single-read libraries of cap-enriched RNA samples were prepared as previously described (Gu et al. 2012). Samples were treated with 0.1 U/ul terminator exonuclease (Epicentre) to degrade 5.8S, 18S, and 26S rRNA. 5S rRNA and tRNA was dephosphorylated with 20 U of CIP (NEB). RNA samples were simultaneously treated with 5 U of DNase I (NEB) to remove any residual DNA contamination. Proteins were removed with PCI extraction in phase-lock tubes (5 Prime) and RNA was precipitated with isopropanol. To remove the 5' cap, RNA was treated with 0.25 U/ul tobacco acid pyrophosphatase (TAP; Epicentre) and purified with PCI extraction and isopropanol precipitation. Individual 5' linkers with 4nt barcodes were then added to the decapped RNA using 2 U/ul of T4 RNA ligase followed by purification. First strand cDNA was then generated using random priming with the addition of a 3' linker sequence using 5 U/ul Superscript III (Invitrogen). cDNA was treated with RNase A/T1 (Ambion) and RNase H (NEB) to remove any RNA contamination. To increase the amount of cDNA, a linear PCR of 10 cycles was performed using a primer specific to the shared 5' linker sequence. To size select, cDNA was separated on a 15% acrylamide TBE denaturing gel (BioRad), visualized with SYBRGold (Invitrogen), and extracted (~125-170 nt). The cDNA was eluted in elution buffer (10 mM Tris [pH 7.5], 1 mM EDTA, 300 mM NaCl) overnight in a termomixer. The eluate was filtered through a Spin-X column (Costar) and precipitated. The cDNA was amplified and resolved on a 10% acrylamide TBE native gel and gel purified. The integrity of the libraries were confirmed by sequencing ~10 fragments from each library. Barcoded libraries were pooled together and sequenced in a single lane using single-read sequencing (100 bp) on an Illumina HiSeq2000 at the UMass Medical School deep sequencing core facility.

Data analysis

Fastq files from single read libraries were collapsed and split based on the 5' barcode in the linker sequence. The 5' barcode and 3' linker sequences were then trimmed from reads and reads were mapped to the mouse mm9 genome using Bowtie1 with reads at

least 19 nt long (although most were 60 nt – 80 nt long). The number of reads for each library is: ESC *EGFP* KD replicate 1 – 22,316,313; ESC *EGFP* KD replicate 2 – 15,969,430; ESC *Smarca4* KD replicate 1 – 11,963,317; ESC *Smarca4* KD replicate 2 – 23,387,852; MEF *EGFP* KD replicate 1 – 20,430,774; MEF *EGFP* KD replicate 2 – 8,441,545; MEF *Smarca4* KD replicate 1 – 21,047,329; MEF *Smarca4* KD replicate 2 – 12,933,820. The mutation rate allowed for the alignment was 0 for reads 19-24 nt, 1 for 25-29 nt, 2 for 30-39 nt, 3 for 40-49 nt, 4 for 50-59 nt, and 5 for 60-69 nt, and 6 for 70 nt or bigger. Reads were separated into RNA classes including: coding, lincRNAs, miRNAs, piRNAs, and “structural” RNAs (tRNAs, rRNAs, snRNAs, and snoRNAs) based on Ensembl data, miRBase 18 and noncoding RNA database fRNAdb 2.4 (Mituyama et al. 2009). Read counts were normalized to parts per million non-structural RNA reads and a gff2 file was generated to visualize alignments on a Genome Browser Gbrowse 1.70 (Stein et al. 2002).

To map reads based on TSS location, a custom PERL script was used to search an interval of 2000 nt upstream to 500 nt downstream of a given read for the nearest gene. Based on the orientation of the 3' end of the CapSeq read, the read was assigned as either sense or antisense to the TSS, and the relative position between the CapSeq 5' end and the start site of the gene was output, where a negative number indicates the CapSeq 5' end is upstream of a gene. Antisense reads were then binned over 500 nt upstream to 100 nt downstream of the annotated TSS, averaged for the two CapSeq libraries, and called if there were 5 reads or more for one of the KD datasets. The reads from these libraries were then sorted by lowest to highest *Smarca4* KD ESCs and visualized through Java TreeView (Saldanha 2004).

To map reads based on DHS location, a custom PERL script was used to search an interval of 500 nt upstream to 500 nt downstream of a given read for the nearest gene, using the DHS locations obtained from the ENCODE data set (GSM1014154) with TSS locations removed. Using all reads called in this interval, similar analysis was performed as described above for antisense reads initiating from annotated TSSs.

To map reads within coding genes, a custom PERL script was used to search an interval of 500 nt downstream to 2000 nt downstream of annotated TSS locations for a given read for the nearest gene. Based on the orientation of the 3' end of the CapSeq read, the read was assigned as either sense or antisense to the coding gene. Using the sense and antisense reads as separate groups, similar analysis was performed as described above.

To map reads based on TTS location, a custom PERL script was used to search an interval of 300 nt upstream to 300 nt downstream of a given read for the nearest TTS. Based on the orientation of the 3' end of the CapSeq read, the read was assigned as either sense or antisense to the TTS. Using only the antisense reads, similar analysis was performed to that described above.

To analyze changes in transcription start site usage, only uniquely mapped, 5' perfectly matched, CapSeq reads of at least 30 nt were included in this analysis. RNA reads were normalized to 10 million sense protein coding reads, and a histogram for the 5' ends of mapped reads was generated for each sample. Sites with less than 5 reads were removed and sites were also removed if they were at least 10-fold less than the upstream or downstream neighboring gene as these sites could be generated by sequencing errors of the nearby abundant reads.

To compare antisense TSS CapSeq reads with MNase-Seq reads upstream of the NDR, CapSeq reads arising in the antisense direction from 500 nt upstream to 100 nt downstream of annotated TSSs were called if there were 5 or more reads in the averaged *EGFP* KD or *Smarca4* KD ESC CapSeq datasets for which there were also MNase-Seq reads. MNase-Seq reads were averaged -500 bp to -200 bp upstream of the annotated TSS for either *EGFP* KD or *Smarca4* KD. For both the CapSeq and MNase-Seq datasets, the *Smarca4* KD data was divided by the *EGFP* KD data, and the \log_2 (ratio) was calculated. The data was clustered using Cluster 3.0 (de Hoon et al. 2004) and visualized by Java TreeView (Saldanha 2004).

Whole-transcript, strand-specific RNA-Seq

Library construction

Strand-specific RNA-Seq libraries were prepared similarly to Kumar et al, with modifications (Levin et al. 2010; Kumar et al. 2012). Briefly, 5 μ g of total RNA was depleted of rRNA using a Ribo-Zero Gold kit (Epicentre) and first strand cDNA was made using 200 ng RNA, 3 μ g random hexamers, 1 μ g Superscript III, and standard dNTPs in the presence of Actinomycin D. First strand cDNA was purified by PCI extraction, ethanol precipitated, and resuspended in water. Second strand cDNA was synthesized with *E. coli* DNA polymerase, in the presence of *E. coli* DNA ligase and RNase H (all from NEB), using dNTPs in which dUTP was substituted for dTTP, at 16°C for 2 hrs. After purification on a Clean and Concentrate column (Zymo Research), cDNA was fragmented using Fragmentase (NEB), PCI extracted and precipitated as above. End repair, A-tailing, and barcoded adapter ligation were performed as described (Illumina), and the second strand cDNA was digested with USER enzyme (NEB). Libraries were amplified from the resulting adapter-ligated first-strand cDNA using Phusion (NEB) and 16 cycles of amplification. Libraries were size-selected on 1.5% agarose gels to a size range of ~180-250 bp. The integrity of the libraries were confirmed by sequencing ~10 fragments from each library. Libraries were combined and sequenced (single read 50 bp with direction corresponding to the first strand cDNA) on a single lane of an Illumina HiSeq2000 at the UMass Medical School deep sequencing core facility.

Data analysis

Fastq files from single read libraries were collapsed and split based on the 5' barcode in the linker sequence. The 5' barcode sequences were then trimmed from reads and reads were mapped to the mouse mm9 genome using Bowtie1 with reads at least 19 nt long. Read counts were normalized to parts per million reads. The number of reads for each library is: *EGFP* KD replicate 1 – 26,490,423; *EGFP* KD replicate 2 – 23,440,035; *Smarca4* KD replicate 1 – 25,155,038; *Smarca4* KD replicate 2 – 14,990,552.

To map reads based on TSS location, a custom PERL script was used to search an interval of 2000 nt upstream to 500 nt downstream of a given read for the nearest gene. Antisense reads were then binned, averaged for the two RNA-Seq libraries, and called if there were 5 reads or more for one of the KD datasets. The reads from these libraries were then sorted from lowest to highest in *Smarca4* KD and visualized through Java TreeView (Saldanha 2004). To map reads based on DHS location, a custom PERL script was used to search an interval of 1000 nt upstream to 1000 nt downstream

of a given read for the nearest gene. All reads were then binned, averaged for the two RNA-Seq libraries, and called if there were 5 reads or more for one of the KD datasets. The reads from these libraries were clustered using Cluster 3.0 (de Hoon et al. 2004) and visualized through Java TreeView (Saldanha 2004). The DEseq software package (Anders and Huber, 2010) was used to identify transcripts whose levels were significantly altered upon *Smarca4* KD, and the pROC package (Robin et al. 2011) was used to create ROC curves.

Generation of nucleosome superbinder lines.

Using the CRISPR/Cas9 system to stimulate recombination (Cong et al. 2013), the nucleosome superbinder sequence (Wang et al. 2011b) was inserted flanking DHS-chr2, in the -1 nucleosome position, and -60, +60, and +180 bp shifted from the -1 nucleosome of the *Ttc25* gene.

To generate the donor plasmid for the DHS-chr2 SB lines, a synthetic sequence for the superbinder was generated (IDT) and its sequence confirmed. This sequence was cloned into the TOPO TA vector (Invitrogen) and sequenced to validate proper ligation.

To generate the donor plasmids for the *Ttc25* SB lines, synthetic sequences in which the superbinder replaced the endogenous sequence at each location were generated (Invitrogen) and their sequences confirmed. These sequences were cloned into a pBlueScript vector containing ~1400 bp of WT *Ttc25* promoter region. For each construct, the PstI-PstI fragment of the homology region was replaced with the PstI-PstI fragment of each synthetic DNA, creating constructs in which the superbinder sequence was surrounded by ~600 bp of endogenous sequence on each side to serve as homology arms for recombination. The plasmid was sequenced to confirm ligation in the proper orientation.

A CRISPR/guideRNA plasmid specific for either DHS-chr2 or *Ttc25* was generated by phosphorylating and annealing oligonucleotides (see Table S1) targeting the region flanking DHS-chr2 or upstream of the *Ttc25* promoter containing a G followed by 19 additional bases of the guide strand plus sticky ends, ligating into a variant of the pX330 plasmid (Cong et al. 2013) into which we inserted a puromycin-resistance cassette.

In a 6-well plate, 2×10^5 E14 ES cells were seeded 24 h prior to transfection. Cells were transfected with 3 μ g of the CRISPR/guideRNA plasmid and 3 μ g of the donor plasmid using 24 μ L of FuGENE HD (Promega) in 100 μ L of OptiMEM. 12 h post transfection cells were split onto three 10 cm plates at clonal density. 48 h post transfection DMEM containing 2 μ g/mL puromycin was added for 40 h. Media was then removed, cells were washed with 1XPBS, and fresh media without puromycin was added. 8 days post transfection, clones were picked, trypsinized, and grown in 96-well plates for ~2 days. After splitting clones into multiple 96 well plates, genomic DNA was isolated from one, and the DHS-chr2 or *Ttc25* promoter region was amplified and digested using SacII. In the superbinder knock-in strains, there is a unique SacII site. The digestion was visualized on a 1% agarose gel, and the PCR from homozygote or heterozygote candidates was cloned using TOPO TA cloning (Invitrogen) and sent for individual sequencing to validate the integration of the superbinder nucleosome into one or both chromosomal copies.

SUPPLEMENTAL FIGURE LEGENDS

Supplemental Figure 1. Widespread upregulation of ncRNAs in *Smarca4* KD cells.

(A) Efficient KD of *Smarca4* in ESCs is confirmed by random primed RT-qPCR with expression levels normalized to GAPDH and shown relative to *EGFP* KD. Shown are the mean +/- SD values of three biological replicates after acute (48 hour) KD. (B) Efficient KD of *Smarca4* is confirmed by Western blotting, where actin serves as a loading control. (C) Levels of Brg1, Oct4, and Nanog in *EGFP* KD and *Smarca4* KD ESCs were confirmed by Western blotting, where actin serves as a loading control. (D) Staining of ESCs for alkaline phosphatase, a marker for pluripotent stem cells, after *EGFP* or *Smarca4* KD. (E-G) Validation of CapSeq and whole-transcript RNA-Seq datasets. (E) Upregulation of antisense transcripts upstream of nine coding genes were confirmed with strand-specific RT-qPCR. Shown are the mean +/- SD values of three biological replicates relative to *EGFP* KD. (F) Validation of RNA-Seq data by random primed RT-qPCR shows an increase in antisense transcript production from 14 coding gene promoters, but not four control locations, in *Smarca4* KD cells. (G) Oligo-dT primed RT-qPCR (expression levels shown as in (F)) shows that antisense transcripts increased upon *Smarca4* KD are polyadenylated. (H) Efficient KD of *Smarca4*, *Smarcc1*, and *Smarcd1* in ESCs is confirmed by random primed RT-qPCR. Expression levels are shown as in (A). For all RT-qPCR analyses, statistical significance is indicated with an asterisk (* $p < 0.05$, ** $p < 0.01$, ns=not significant).

Supplemental Figure 2. Comparison of ncRNAs in ESCs and MEFs from CapSeq data.

(A-H) Violin plots quantifying noncoding transcripts surrounding DHSs (+/- 500 bp) (A), TSSs (-500 to +100 bp) (B), intragenic regions (>500 bp from TSS) (C), or TTSs (-500 bp to +500 bp from TTS) (D) in averaged biological replicates of *EGFP* KD and *Smarca4* KD ESC and MEF CapSeq experiments. (E-H) Heatmaps quantifying noncoding transcripts surrounding DHSs (+/- 500 bp) (E), TSSs (-500 to +100 bp) (F), intragenic regions (antisense only, > 500 bp from TSS) (G), or TTSs (antisense only, -500 to +500 bp from TTS) (H) in WT ESC and embryoid body (EB) CapSeq experiments. Expression is indicated as \log_2 (normalized reads).

Supplemental Figure 3. Altered positioning of transcription start sites in ESCs upon *Smarca4* KD.

(A-C) TSS positions from *EGFP* KD (A) or *Smarca4* KD (B) ESC CapSeq data are plotted relative to the annotated TSS. The shaded area indicates the variance between the two replicates. (C) Overlay of *EGFP* KD and *Smarca4* KD ESC start site data shown in (A-B). (D-F) TSS positions from *EGFP* KD (D) or *Smarca4* KD (E) MEF CapSeq data are plotted as in A. (F) Overlay of *EGFP* KD and *Smarca4* KD MEF start site data. A K-S test demonstrated statistically significant differences between KDs. (p-value ESC *EGFP* KD vs *Smarca4* KD = $1.532e-14$; p-value MEF *EGFP* KD vs *Smarca4* KD = $1.371e-7$). (E) Genome browser tracks of two coding genes with altered start sites in ESCs. Isoforms are shown in an orange box below the scale, with introns indicated as black lines. Browser tracks of normalized CapSeq reads of one replicate from *EGFP* KD

and *Smarca4* KD are shown in log₂ scale. Blue bars indicate transcription from the Crick strand, while red bars indicate transcription from the Watson strand. The number of normalized reads for each sample is indicated.

Supplemental Figure 4. ncRNA expression is altered more at esBAF occupied regions.

(A-D) Histogram of normalized transcripts obtained from RNA-Seq analysis surrounding the DHSs (A-B) and TSSs (C-D) in *EGFP* KD and *Smarca4* KD ESCs. Transcripts are sorted by esBAF bound (A and C) or esBAF unbound (B and D) regions.

Supplemental Figure 5. esBAF regulates the expression of many more ncRNAs than mRNAs in ESCs.

(A) Table indicating the number of ncRNAs or mRNAs altered in *Smarca4* KD relative to *EGFP* KD control ESCs. (B) Heatmap quantifying mRNA transcripts in *EGFP* KD and *Smarca4* KD RNA-Seq experiments. Expression is indicated as log₂(normalized reads). (C-E) Scatterplot showing the correlation between sense (mRNA) and as-TSS transcripts in *EGFP* KD (C), *Smarca4* KD (D), or log₂ (*Smarca4* KD/*EGFP* KD) (E).

Supplemental Figure 6. Independent esiRNA confirms changes in ncRNA expression upon *Smarca4* KD.

(A) Efficient KD of *Smarca4* with independent esiRNAs in ESCs is confirmed by random primed RT-qPCR with expression levels normalized to GAPDH and shown relative to *EGFP* KD. Shown are the mean +/- SD values of three biological replicates. (B-C) Validation of RNA-Seq data by random primed RT-qPCR using independent esiRNAs to *Smarca4* at DHSs (B) or antisense to TSSs (C). Significance is indicated with an asterisk (*p<0.05, **p<0.01, ns=not significant).

Supplemental Figure 7. ncRNAs are increased upon *Smarca4* KD in ESCs but not MEFs.

(A) Efficient KD of *Smarca4* in MEFs is confirmed by random primed RT-qPCR with expression levels shown relative to *EGFP* KD. (B) *Smarca4* KD is confirmed by Western blotting, where actin serves as a loading control. (C) Validation of MEF CapSeq datasets. Levels of antisense transcripts produced upstream of coding genes were confirmed with random primed RT-qPCR on *EGFP* KD and *Smarca4* KD cells. Expression levels are shown relative to the *EGFP* KD. Shown are the mean +/- SD values of three biological replicates. (D-E) Genome browser tracks of two DHSs (D) and two coding genes (E) in *EGFP* KD and *Smarca4* KD MEFs, as in Fig. 1. (F) Histone H3 levels were determined in *EGFP* KD and *Smarca4* KD MEFs by ChIP-qPCR over the -1 nucleosome. Significance is indicated with an asterisk (*p<0.05, **p<0.01, ns=not significant).

Supplemental Figure 8. Alterations in nucleosome occupancy upon *Smarca4* KD, sorted by gene expression.

(A) Bioanalyzer traces of *EGFP* KD and *Smarca4* KD MNase digested samples used for library construction. (B) Aggregation plots comparing nucleosome occupancy in control (*EGFP*) KD and KD of the Mbd3/NuRD component *Mbd3* at DHSs. (C-G)

Aggregation plots of the relative nucleosome occupancy obtained from the MNase-Seq data upon *EGFP* KD or *Smarca4* KD over TSSs +/- 2 kb in ESCs. Plots are sorted by gene expression in ESCs (GSM521650), broken into quintiles from highest (C) to lowest (G).

Supplemental Figure 9. Validation of nucleosome changes around TSSs.

(A-B) Histone H3 levels were determined in *EGFP* KD and *Smarca4* KD ESCs by ChIP-qPCR over the -1 nucleosome (A) or +1 nucleosome (B) of genes found to be altered in the *Smarca4* KD MNase-Seq dataset. Histone H3 levels are expressed as a fraction of the input. Shown are the mean +/- SD values of three biological replicates. (C)

Validation of alterations in nuclease accessibility over NDRs near TSSs. Accessibility to MNase treatment was determined in *EGFP* KD and *Smarca4* KD ESCs by MNase-qPCR over the NDR of genes found to be altered in the *Smarca4* KD MNase-Seq dataset. Relative protection from undigested chromatin is shown as the mean +/- SD values of three replicates. Significance is indicated with an asterisk (* $p < 0.05$, ** $p < 0.01$, ns=not significant).

Supplemental Figure 10. Nucleosome occupancy is altered more at genes bound and/or regulated by esBAF upon *Smarca4* KD.

Aggregation plots of relative nucleosome occupancy upon *EGFP* KD or *Smarca4* KD over TSSs +/- 2 kb in ESCs. (A-E) Plots are sorted by *Smarca4* KD gene expression, obtained from published microarray data (Yildirim et al. 2011). Reads are sorted by the top 20% of ESC genes upregulated in the KD datasets (A) through the 20% of genes most downregulated in the KD datasets (E), with the remaining 60% of genes broken into three intermediate classes of expression. (F-H) Plots are sorted by Brg1 occupancy, obtained from published ChIPseq data (Yildirim et al. 2011; Ho et al. 2009a). Reads are sorted by the genes with the most occupancy (F), intermediate occupancy (G) and lowest occupancy (H).

Supplemental Figure 11. Confirmation of superbinder positioning flanking a DHS.

(A) Diagram of the DHS locus with qPCR amplicons for panels (D) and (E) depicted. (B) Efficient KD of *Smarca4* in WT and SB ESCs is confirmed by random primed RT-qPCR with expression levels shown relative to *EGFP* KD. (C) *Smarca4* KD is confirmed by Western blotting, where actin serves as a loading control. (D) Histone H3 ChIP-qPCR over the WT -1 nucleosome in either *EGFP* KD or *Smarca4* KD in WT or SB homozygote (SB/SB) lines. Histone H3 levels in cells knocked down as indicated are expressed as a fraction of the input. Shown are the mean +/- SD values of three replicates. (E) Histone H3 ChIP-qPCR over the SB -1 nucleosome in either *EGFP* KD or *Smarca4* KD in WT or nucleosome SB/SB lines. Histone H3 levels are shown as in (D). Significance is indicated with an asterisk (* $p < 0.05$, ** $p < 0.01$, ns=not significant).

Supplemental Figure 12. Confirmation of superbinder positioning at the -1 nucleosome position of *Ttc25*.

(A) Diagram of the *Ttc25* locus with qPCR amplicons for panels (D) and (E) depicted. (B) Efficient KD of *Smarca4* in WT and SB ESCs is confirmed by random primed RT-qPCR with expression levels shown relative to *EGFP* KD. (C) *Smarca4* KD is confirmed

by Western blotting, where actin serves as a loading control. **(D)** Histone H3 ChIP-qPCR over the WT -1 nucleosome in either *EGFP* KD or *Smarca4* KD in WT or SB heterozygote (+/SB) or homozygote (SB/SB) lines. Histone H3 levels in cells knocked down as indicated are expressed as a fraction of the input. Shown are the mean +/- SD values of three replicates. **(E)** Histone H3 ChIP-qPCR over the SB -1 nucleosome in either *EGFP* KD or *Smarca4* KD in WT or nucleosome +/SB or SB/SB lines. Histone H3 levels are shown as in **(D)**. **(F)** Random primed RT-qPCR in either *EGFP* KD or *Smarca4* KD in WT or nucleosome +/SB or SB/SB lines for as-TSS unlinked to *Ttc25* indicates that knock-in of the SB sequence upstream of the *Ttc25* does not affect unlinked antisense transcripts. Significance is indicated with an asterisk (* $p < 0.05$, ** $p < 0.01$, ns=not significant).

Supplemental Figure 13. Confirmation of superbinder positioning at -60, +60, and +180 relative to the -1 nucleosome position of *Ttc25*.

(A-C) Efficient KD of *Smarca4* in WT or SB/SB ESCs is confirmed by random primed RT-qPCR with expression levels normalized to GAPDH and shown relative to *EGFP* KD. Shown are the mean +/- SD values of three biological replicates. **(D-F)** Histone H3 ChIP-qPCR over the SB -1 nucleosome in either *EGFP* KD or *Smarca4* KD in WT or SB/SB lines. Histone H3 levels in cells knocked down as indicated are expressed as a fraction of the input. Shown are the mean +/- SD values of three replicates. **(G-I)** RNAPII or IgG control ChIP-qPCR upstream of the *Ttc25* locus in WT or SB/SB lines, upon wither *EGFP* KD or *Smarca4* KD, expressed as a fraction of the input. Shown are the mean +/- SD values of three biological replicates. **(J-L)** RNAPII or IgG control ChIP-qPCR over the *Ttc25* locus in WT or SB/SB lines, upon either *EGFP* KD or *Smarca4* KD, expressed as a fraction of the input. Shown are the mean +/- SD values of three biological replicates. Significance is indicated with an asterisk (* $p < 0.05$, ** $p < 0.01$, ns=not significant).

SUPPLEMENTAL TABLES

Supplemental Table 1. Oligonucleotides used in this study.

Name	Sequence	Location/ amplicon product	Purpose
<i>GAPDH</i> F	TTGATGGCAACA ATCTCCAC	chr6:125,113,383- 125,115,326	RT-qPCR for mouse GAPDH
<i>GAPDH</i> R	CGTCCCGTAGAC AAAATGGT	chr6:125,113,383- 125,115,326	RT-qPCR for mouse GAPDH
<i>Smarca4</i> F	GGACAGACACCT GCTATTGGAC	chr9:21,447,163- 21,452,081	RT-qPCR for <i>Smarca4</i>
<i>Smarca4</i> R	GGCTACTTCATA CCCTGGGTTC	chr9:21,447,163- 21,452,081	RT-qPCR for <i>Smarca4</i>
<i>Smarcc1</i> F	GAAGAAGTACCC CTGGAATTGG	chr14:85,158,440- 85,158,626	RT-qPCR for <i>Smarcc1</i>
<i>Smarcc1</i> R	GCTGACCATCAG	chr14:85,158,440-	RT-qPCR for <i>Smarcc1</i>

<i>Smarcd1</i> F	GATCTGTTTC CGAGCGAGAGTT	85,158,626 chr15:99,538,193-99,539,785	RT-qPCR for <i>Smarcd1</i>
<i>Smarcd1</i> R	TGTTCTCTGT GGGTCTTCAGAG	chr15:99,538,193-99,539,785	RT-qPCR for <i>Smarcd1</i>
W-chr3:63099200-63099290 F	TGTCATCCAC ACACGGTGTGAC	chr3:63,099,355-63,099,417	RT-qPCR for DHS W-chr3:63099200-63099290
W-chr3:63099200-63099290 R	AGAGCAGTTCCC TGGGTGAC	chr3:63,099,355-63,099,417	RT-qPCR for DHS W-chr3:63099200-63099290
C-chr3:63099200-63099290 F	GAGGAGAGGAG GGAAGGATG	chr3:63,099,070-63,099,155	RT-qPCR for DHS C-chr3:63099200-63099290
C-chr3:63099200-63099290 R	TCTTGCTCTCTCC GTTTTCC	chr3:63,099,070-63,099,155	RT-qPCR for DHS C-chr3:63099200-63099290
W-chr12:112640141-112640291 F	CTCTCAGGACGA AGCCTCAG	chr12:112,640,255-112,640,317	RT-qPCR for DHS W-12:112640141-112640291
W-12:112640141-112640291 R	TAGCTGCCATCC AAGGTGTT	chr12:112,640,255-112,640,317	RT-qPCR for DHS W-12:112640141-112640291
W-chr16:32502840-32502990 F	AGTGGAATTAGC ATCAAATATAAT CA	chr16:32,502,961-32,503,020	RT-qPCR for DHS W-chr16:32502840-32502990
W-chr16:32502840-32502990 R	TGTATAGAGGAT TGTTGAGGATGG	chr16:32,502,961-32,503,020	RT-qPCR for DHS W-chr16:32502840-32502990
C-chr5:20216700-20216850 F	CATTCCTGCCAA TTCATCCT	chr5:20,216,697-20,216,760	RT-qPCR for DHS C-chr5:20216700-20216850
C-chr5:20216700-20216850 R	ACCCTATCCTGC GTGTCATC	chr5:20,216,697-20,216,760	RT-qPCR for DHS C-chr5:20216700-20216850
C-chr3:34627320-34627470 F	CCTCTCCACATC ATGCCAAG	chr3:34,627,189-34,627,248	RT-qPCR for DHS C-chr3:34627320-34627470
C-chr3:34627320-34627470 R	GGTTTCAGGGTC TTTTCTTTTG	chr3:34,627,189-34,627,248	RT-qPCR for DHS C-chr3:34627320-34627470
W-chr9:63651140-63651290 F	CCCTGTGAATAG TGGGAAA	chr9:63,651,371-63,651,436	RT-qPCR for DHS W-chr9:63651140-63651290
W-chr9:63651140-63651290 R	GAAGGCAGAGAT GGGAAATG	chr9:63,651,371-63,651,436	RT-qPCR for DHS W-chr9:63651140-63651290
W-chr4:153479800-153479950 F	GGTTTGTGGCAC GCATCTA	chr4:153,480,060-153,480,139	RT-qPCR for DHS W-chr4:153479800-153479950

W-chr4:153479800-153479950 R	TACTGGCCCTCT CAGCTTGT	chr4:153,480,060-153,480,139	RT-qPCR for DHS W-chr4:153479800-153479950
C-chr16:94534280-94534430 F	TTGGGGACTGAA CCTAGTCCT	chr16:94,534,037-94,534,100	RT-qPCR for DHS C-chr16:94534280-94534430
C-chr16:94534280-94534430 F	AACCTGGGGTTT ATCTTTAGCC	chr16:94,534,037-94,534,100	RT-qPCR for DHS C-chr16:94534280-94534430
<i>as-Klf11</i> F	CTGCGGATTTGC TCTGGT	chr12:25,336,505-25,336,654	RT-qPCR for antisense transcript
<i>as-Klf11</i> R	TGACGTCATGGC TGGAAATA	chr12:25,336,505-25,336,654	RT-qPCR for antisense transcript
<i>as-Klf11</i> as	TCCCATCTAGTTC CCCCAAT	chr12:25,336,787	primer for antisense cDNA production
<i>as-Klf11</i> s	TAAGTGACGGGG CTGAGCGC	chr12:25,336,434	primer for sense cDNA production
<i>as-Fam155a</i> F	TCCCCTCCTCCT CTCCTC	chr8:9,771,521-9,771,622	RT-qPCR for antisense transcript
<i>as-Fam155a</i> R	GAGAGCCAGCGC GAAGTAG	chr8:9,771,521-9,771,622	RT-qPCR for antisense transcript
<i>as-Fam155a</i> as	CTTCCGACCTAA GCATCAGC	chr8:9,779,210	primer for antisense cDNA production
<i>as-Fam155a</i> s	AAGATGGCGGCA ACTTAGC	chr8:9,778,628	primer for sense cDNA production
<i>as-Echdc1</i> F	GTGTGGAAGCCG GAAGAG	chr10:29,033,068-29,033,159	RT-qPCR for antisense transcript
<i>as-Echdc1</i> R	AGCCCCTGGCTC TGACTT	chr10:29,033,068-29,033,159	RT-qPCR for antisense transcript
<i>as-Echdc1</i> as	GAGGGGGAGGG GACATCT	chr10:290,33,202	primer for antisense cDNA production
<i>as-Echdc1</i> s	CGCCAGAGTTCC TTCAGCTA	chr10:29,032,986	primer for sense cDNA production
<i>as-Gtf3c6</i> F	GGCTGGCAACGC TAAACTAA	chr10:39,978,255-39,978,387	RT-qPCR for antisense transcript
<i>as-Gtf3c6</i> R	CTTCACGCTCAG GAAAGGAC	chr10:39,978,255-39,978,387	RT-qPCR for antisense transcript
<i>as-Rps29</i> F	GGAGTTCTGGGC TGTAGTGC	chr12:70,260,354-70,260,498	RT-qPCR for antisense transcript

<i>as-Rps29</i> R	GTTTTGACCTGC TCCGTTTC	chr12:70,260,354- 70,260,498	RT-qPCR for antisense transcript
<i>as-Ttc25</i> F	TTCTTGGCTTGCT TTGTCTG	chr11:100,406,770- 100,406,854	RT-qPCR for antisense transcript
<i>as-Ttc25</i> R	TCCAGAGTGATC GCTGTTTG	chr11:100,406,770- 100,406,854	RT-qPCR for antisense transcript
<i>as-Ttc25</i> as	TCAGACAAGTGC TGAGCGCG	chr11:100,406,883	primer for antisense cDNA production
<i>as-Ttc25</i> s	TCCTAATGGGAC CTGGAGTG	chr11:100,406,707	primer for sense cDNA production
<i>as-Mcm5</i> F	ACTTGCGATCCT CCTGCTTA	chr8:77,633,101- 77,633,179	RT-qPCR for antisense transcript
<i>as-Mcm5</i> R	CCTTCGGAGAAA ACCTAGCC	chr8:77,633,101- 77,633,179	RT-qPCR for antisense transcript
<i>as-Mcm5</i> as	ATTTTGTGAGGC TGGACGTT	chr8:77,633,267	primer for antisense cDNA production
<i>as-Mcm5</i> s	AGAGGCCAGGAG AGGACATT	chr8:77,632,910	primer for sense cDNA production
<i>as-Med22</i> F	AGAGTCCGAAGT GGGTCCTT	chr2:26,766,219- 26,766,318	RT-qPCR for antisense transcript
<i>as-Med22</i> R	AGGGAATTGTGG GGGATAAG	chr2:26,766,219- 26,766,318	RT-qPCR for antisense transcript
<i>as-Fam46d</i> F	AGTGAGTCGCTT CGGTTAGG	chrX:105,011,709- 105,011,771	RT-qPCR for antisense transcript
<i>as-Fam46d</i> R	CTTCAGCTCTCG GACTCCAC	chrX:105,011,709- 105,011,771	RT-qPCR for antisense transcript
<i>as-Ssr4</i> F	GGGTATGGGTTG AGAAAACG	chrX:71,032,271- 71,032,330	RT-qPCR for antisense transcript
<i>as-Ssr4</i> R	GCGTAAGAACCG GTGTGACT	chrX:71,032,271- 71,032,330	RT-qPCR for antisense transcript
<i>as-1110038D17Rik</i> F	CCTTCCACCCCC ACTTCT	chr10:74,980,179- 74,980,239	RT-qPCR for antisense transcript
<i>as-1110038D17Rik</i> R	GAGCGTTTCAGG GAAGGAC	chr10:74,980,179- 74,980,239	RT-qPCR for antisense transcript
<i>as-1110038D17Rik</i> as	GCCTAATCCCTT CCAGGTCT	chr10:74,980,460	primer for antisense cDNA production
<i>as-1110038D17Rik</i> s	GGAGAACCAGAG CTTCCATCT	chr10:74,980,658	primer for sense cDNA production

<i>as-Trappc9</i> F	GAAACAAGCACA CTCCCAGTC	chr15:72,894,962- 72,895,036	RT-qPCR for antisense transcript
<i>as-Trappc9</i> R	GGTCAAGGGGCT CCATCTA	chr15:72,894,962- 72,895,036	RT-qPCR for antisense transcript
<i>as-Trappc9</i> as	CGAAGAGCGCAG AAACCTT	chr15:72,898,600	primer for antisense cDNA production
<i>as-Trappc9</i> s	GGCCCACTCTGG TGTTTCT	chr15:72,897,099	primer for sense cDNA production
<i>as-Napepld</i> F	CACTGTGGGTGT TTGTGAGC	chr5:21,201,414- 21,201,503	RT-qPCR for antisense transcript
<i>as-Napepld</i> R	GGCTCAGCAGGT AAGAGCAC	chr5:21,201,414- 21,201,503	RT-qPCR for antisense transcript
<i>as-St6galnac6</i> F	CCTACACATAGG TCCACACACA	chr2:32,463,313- 32,460,642	RT-qPCR for antisense transcript
<i>as-St6galnac6</i> R	CCAAGTGCTGGG ATTAAAGG	chr2:-32,463,313- 32,460,642	RT-qPCR for antisense transcript
<i>as-Eya3</i> F	AGTTCCCGACGG CTCTGAT	chr4:132,478,569- 132,478,652	RT-qPCR for antisense transcript
<i>as-Eya3</i> R	GCGTGACTGCGC TTTACATA	chr4:132,478,569- 132,478,652	RT-qPCR for antisense transcript
<i>as-Plod1</i> F	CCCCGCTTCTCT CCAAGT	chr4:147,311,018- 147,311,097	RT-qPCR for antisense transcript
<i>as-Plod1</i> R	ATCGCGGTGCAG ATGATATT	chr4:147,311,018- 147,311,097	RT-qPCR for antisense transcript
<i>as-Plod1</i> as	GGGAAGGGTTTT CCTGCTTA	chr4:147,313,950	primer for antisense cDNA production
<i>as-Plod1</i> s	ACCATCACCACA CACACACA	chr4:147,313,644	primer for sense cDNA production
<i>as-Parp4</i> F	CCCCTTTGGGAA ATTTGTTT	chr14:57,194,157- 57,194,250	RT-qPCR for antisense transcript
<i>as-Parp4</i> R	GGATGGGGACTT TTGACAGA	chr14:57,194,157- 57,194,250	RT-qPCR for antisense transcript
<i>as-Zfp62</i> F	TCAGCTTCACAA GCAGGAAG	chr11:49,016,720- 49,016,829	RT-qPCR for antisense transcript
<i>as-Zfp62</i> R	GGGGTTCTAGT TGTCTTGA	chr11:49,016,720- 49,016,829	RT-qPCR for antisense transcript
<i>as-Mrps15</i> F	GCTGGGATTTGA ACTCAGGA	chr4:125,723,694- 125,723,755	RT-qPCR for antisense transcript

<i>as-Mrps15</i> R	AAATGGCTCAGC GGTTAAGA	chr4:125,723,694- 125,723,755	RT-qPCR for antisense transcript
<i>as-Cyp2d34</i> F	CCACCAACCTCA TTCCTTTG	chr15:82,451,437- 82,451,541	RT-qPCR for antisense transcript
<i>as-Cyp2d34</i> R	ATGTTTCAGCCCA GCAGAATC	chr15:82,451,437- 82,451,541	RT-qPCR for antisense transcript
<i>as-Gdf6</i> F	GGTCCCTGGAGA AGTTTCGAG	chr4:9,771,174- 9,771,268	RT-qPCR for antisense transcript
<i>as-Gdf6</i> R	CCTCTGTCCCAG GGTTGG	chr4:9,771,174- 9,771,268	RT-qPCR for antisense transcript
<i>as-Tas2r140</i> F	GCACACACAACA GCCAGAAG	chr6:133,006,040- 133,006,127	RT-qPCR for antisense transcript
<i>as-Tas2r140</i> R	TTGGAGTATCTTT GTTTTGCTGA	chr6:133,006,040- 133,006,127	RT-qPCR for antisense transcript
<i>as-Tas2r140</i> as	ACCAGGAGATGC TCCAAGTC	chr6:133,006,488	primer for antisense cDNA production
<i>as-Tas2r140</i> s	TGAAAATAAGATA AGGTCACCTAAC A	chr6:133,006,029	primer for sense cDNA production
<i>Arih2</i> F	CAGGTCAAGCCA GACCAAAC	chr9:108,551,604- 108,551,700	ChIP-qPCR primer for +1 nucleosome confirmation
<i>Arih2</i> R	CTCTGCCGGAGG AAGCTG	chr9:108,551,604- 108,551,700	ChIP-qPCR primer for +1 nucleosome confirmation
<i>Ywhaz</i> F	ACCGACCCTTTT AGGTCCTG	chr15:36,724,210- 36,724,272	ChIP-qPCR primer for +1 nucleosome confirmation
<i>Ywhaz</i> R	CAGCTAGAGCCC TAGGAACG	chr15:36,724,210- 36,724,272	ChIP-qPCR primer for +1 nucleosome confirmation
<i>Ppm1j</i> F	ATCTGCCCAACG CTACCTC	chr3:104,584,084- 104,584,146	ChIP-qPCR primer for +1 nucleosome confirmation
<i>Ppm1j</i> R	TCTCCCGGGAAC TCTTAGGT	chr3:104,584,084- 104,584,146	ChIP-qPCR primer for +1 nucleosome confirmation
<i>Expi</i> F	CCAGTCAGAGCC AACATGAA	chr11:83,522,605- 83,522,693	ChIP-qPCR primer for +1 nucleosome confirmation
<i>Expi</i> R	TTAGACAGAGCC CAGGCAGT	chr11:83,522,605- 83,522,693	ChIP-qPCR primer for +1 nucleosome confirmation
<i>Traf3ip3</i> F	GTTATTTTCGCAC AGCAGCA	chr1:195,027,639- 195,027,728	ChIP-qPCR primer for +1 nucleosome confirmation
<i>Traf3ip3</i> R	TCAAATTGCTAAG GGCAAGG	chr1:195,027,639- 195,027,728	ChIP-qPCR primer for +1 nucleosome confirmation
<i>Coasy</i> F	CGGTTTCAGCCTA ACAAGAGG	chr11:100,944,103- 100,944,168	ChIP-qPCR primer for +1 nucleosome confirmation
<i>Coasy</i> R	CCAGGAACCCCT	chr11:100,944,103-	ChIP-qPCR primer for +1

	GAGTCAT	100,944,168	nucleosome confirmation
<i>Cd48</i> F	AAAACAGGGATG GTGTCTGG	chr1:173,612,236- 173,612,296	ChIP-qPCR primer for +1 nucleosome confirmation
<i>Cd48</i> R	TTGAAATCCAGTT CCCAAGG	chr1:173,612,236- 173,612,296	ChIP-qPCR primer for +1 nucleosome confirmation
<i>Dad1</i> F	CGAGGAGACAGT AGCCGAAC	chr14:54,873,376- 54,873,446	ChIP-qPCR primer for +1 nucleosome confirmation
<i>Dad1</i> R	GAAGTTGCTGGA CGCCTATC	chr14:54,873,376- 54,873,446	ChIP-qPCR primer for +1 nucleosome confirmation
<i>Acot7</i> F	GCTGGGACAGAC AAGAGGTC	chr4:151,559,714- 151,559,776	MNase-qPCR primer for NDR nucleosome confirmation
<i>Acot7</i> R	TCCCTCCCATA GCTCCTAC	chr4:151,559,714- 151,559,776	MNase-qPCR primer for NDR nucleosome confirmation
<i>Rin2</i> F	CTCTTGCAACCAG GTGTGTGT	chr2:145,611,255- 145,611,317	MNase-qPCR primer for NDR nucleosome confirmation
<i>Rin2</i> R	CACCCTGCAAAG ACTTCCAT	chr2:145,611,255- 145,611,317	MNase-qPCR primer for NDR nucleosome confirmation
<i>Zwilch</i> F	TCACGCTTTAAGT TCGGTTTG	chr9:64,020,774- 64,020,877	MNase-qPCR primer for NDR nucleosome confirmation
<i>Zwilch</i> R	CCCCTAACAGAA ATGGGAGA	chr9:64,020,774- 64,020,877	MNase-qPCR primer for NDR nucleosome confirmation
<i>Pank1</i> F	GGTCTGAAGGGA GGGAAGAG	chr19:34,953,947- 34,954,036	MNase-qPCR primer for NDR nucleosome confirmation
<i>Pank1</i> R	GAGTGTGCCAAC CAAGGAAT	chr19:34,953,947- 34,954,036	MNase-qPCR primer for NDR nucleosome confirmation
<i>Rnaseh2b</i> F	AGCCAATTTGAA GGCTGCT	chr14:62,950,721- 62,950,824	MNase-qPCR primer for NDR nucleosome confirmation
<i>Rnaseh2b</i> R	TGTGGAGCTCCT CGTTTTTC	chr14:62,950,721- 62,950,824	MNase-qPCR primer for NDR nucleosome confirmation
<i>Grhl2</i> F	GTCAGCTCGCAG AGTCTCCA	chr15:37,162,616- 37,162,689	MNase-qPCR primer for NDR nucleosome confirmation
<i>Grhl2</i> R	CTCCAAGTGCAG GTCACTCA	chr15:37,162,616- 37,162,689	MNase-qPCR primer for NDR nucleosome confirmation
<i>Olf1450</i> F	GCCTTATGCAGT CTGGGAAA	chr19:13,027,996- 13,028,099	MNase-qPCR primer for NDR nucleosome confirmation
<i>Olf1450</i> R	TGCTGTTGGCCA CATACATT	chr19:13,027,996- 13,028,099	MNase-qPCR primer for NDR nucleosome confirmation

<i>Cd5l</i> F	CAGTCACCTCCC TTCCTCTG	chr3:87,161,725- 87,161,789	MNase-qPCR primer for NDR nucleosome confirmation
<i>Cd5l</i> R	AGGGGGTGGGA CTGATAGAG	chr3:87,161,725- 87,161,789	MNase-qPCR primer for NDR nucleosome confirmation
<i>Serpina6</i> F	AAGCATCAACCA ATGGGAAG	chr12:104,895,423- 104,895,499	MNase-qPCR primer for NDR nucleosome confirmation
<i>Serpina6</i> R	CATGCAATGTCG AGCTGATT	chr12:104,895,423- 104,895,499	MNase-qPCR primer for NDR nucleosome confirmation
<i>Mrps15</i> F	AACTCCAGAAC AGGGCATC	chr4:125,723,636- 125,723,707	ChIP-qPCR primer for -1 nucleosome confirmation
<i>Mrps15</i> R	GTTCAAATCCCA GCAACCAC	chr4:125,723,636- 125,723,707	ChIP-qPCR primer for -1 nucleosome confirmation
<i>Ednrb</i> F	TTTGGGGAAGTT GTCTTTCG	chr14:104,243,885- 104,243,974	ChIP-qPCR primer for -1 nucleosome confirmation
<i>Ednrb</i> R	CCTGCATGCTGG CTTAAAAC	chr14:104,243,885- 104,243,974	ChIP-qPCR primer for -1 nucleosome confirmation
<i>Pak6</i> F	CCCGACGATATC AAAATTGC	chr2:118,488,983- 118,489,081	ChIP-qPCR primer for -1 nucleosome confirmation
<i>Pak6</i> R	GCTCACTTTGGG ATTTCTCC	chr2:118,488,983- 118,489,081	ChIP-qPCR primer for -1 nucleosome confirmation
<i>Grip1</i> F	ATCTCTCGCCTTT CCTGTGA	chr10:119,256,137- 119,256,216	ChIP-qPCR primer for -1 nucleosome confirmation
<i>Grip1</i> R	CTGTGCATTCTA GCCAGTGC	chr10:119,256,137- 119,256,216	ChIP-qPCR primer for -1 nucleosome confirmation
<i>Rab38</i> F	GGGAGGCGAGA GAAAAATCT	chr7:95,578,600- 95,578,674	ChIP-qPCR primer for -1 nucleosome confirmation
<i>Rab38</i> R	CCAGTGCTACTG CCTGTCAA	chr7:95,578,600- 95,578,674	ChIP-qPCR primer for -1 nucleosome confirmation
<i>Ift74</i> F	GGGTTCGATTGG AACTAGCA	chr4:94,280,670- 94,280,742	ChIP-qPCR primer for -1 nucleosome confirmation
<i>Ift74</i> R	GATTGCATTGGT TCCTCCAG	chr4:94,280,670- 94,280,742	ChIP-qPCR primer for -1 nucleosome confirmation
<i>Ghr</i> F	ATAGGCTGGCCT CAAACCTCA	chr15:3,421,886- 3,421,960	ChIP-qPCR primer for -1 nucleosome confirmation
<i>Ghr</i> R	TGGTGTGGTAC ACCCCTTT	chr15:3,421,886- 3,421,960	ChIP-qPCR primer for -1 nucleosome confirmation
<i>Trp53i11</i> F	AGGCATGGGACA GGTTGTAG	chr2:93,026,961- 93,027,037	ChIP-qPCR primer for -1 nucleosome confirmation

<i>Trip53i11</i> R	CCAAGAGAGAGT CCCAGGTG	chr2:93,026,961- 93,027,037	ChIP-qPCR primer for -1 nucleosome confirmation
<i>Arhgap15</i> F	GGCATTCTGAGC AACTCTCC	chr2:43,603,771- 43,603,843	ChIP-qPCR primer for -1 nucleosome confirmation
<i>Arhgap15</i> R	TGCAGATGCACC AGAACTTT	chr2:43,603,771- 43,603,843	ChIP-qPCR primer for -1 nucleosome confirmation
<i>Zfp595</i> F	TTGTCTTGCAGC ATCTCAGG	chr13:67,433,912- 67,433,993	ChIP-qPCR primer for -1 nucleosome confirmation
<i>Zfp595</i> R	GCAGTGCTCAGA AACCACCT	chr13:67,433,912- 67,433,993	ChIP-qPCR primer for -1 nucleosome confirmation
C-chr5:119290080- 119290230 F	GCTGTGACAGAA TGCCTGAA	chr5:119,289,895- 119,289,971	ChIP-qPCR primer for flanking DHS nucleosome occupancy confirmation
C-chr5:119290080- 119290230 R	GCCACCATGGAC TGAAACT	chr5:119,289,895- 119,289,971	ChIP-qPCR primer for flanking DHS nucleosome occupancy confirmation
W-chr5:119290080- 119290230 F	GTGCTGAGGAGG TCAAAGG	chr5:119,290,286- 119,290,359	ChIP-qPCR primer for flanking DHS nucleosome occupancy confirmation
W-chr5:119290080- 119290230 R	CACGGTGATTCA CAACTGCT	chr5:119,290,286- 119,290,359	ChIP-qPCR primer for flanking DHS nucleosome occupancy confirmation
C-chr3:30600200- 30600350 F	CCCGCTCTGCAA AACATAGT	chr3:30,599,981- 30,600,050	ChIP-qPCR primer for flanking DHS nucleosome occupancy confirmation
C-chr3:30600200- 30600350 R	TCTCACCGGTGC TGTGTTAC	chr3:30,599,981- 30,600,050	ChIP-qPCR primer for flanking DHS nucleosome occupancy confirmation
W-chr3:30600200- 30600350 F	TGGCTCTAAGCT GAGAAGTGG	chr3:30,600,502- 30,600,576	ChIP-qPCR primer for flanking DHS nucleosome occupancy confirmation
W-chr3:30600200- 30600350 R	TTGTGGAGAGTC CTCAGGAAG	chr3:30,600,502- 30,600,576	ChIP-qPCR primer for flanking DHS nucleosome occupancy confirmation
W-chr12:78090160- 78090310 F	TCTCCATCAGATT GGCTGGT	chr12:78,090,519- 78,090,589	ChIP-qPCR primer for flanking DHS nucleosome occupancy confirmation
W-chr12:78090160- 78090310 R	GGCCCTTTCTCC ATCAATTA	chr12:78,090,519- 78,090,589	ChIP-qPCR primer for flanking DHS nucleosome occupancy confirmation
W- chr11:117495120- 117495270 F	GATCAGGCGTTG GTAGAGGA	chr11:117,495,423- 117,495,502	ChIP-qPCR primer for flanking DHS nucleosome occupancy confirmation
W- chr11:117495120- 117495270 R	GGTCATCGGCTT AAGTTCCA	chr11:117,495,423- 117,495,502	ChIP-qPCR primer for flanking DHS nucleosome occupancy confirmation
W-chr10:95182920- 95183070 F	CATGGCTGTTTC CTTGACCT	chr10:95,183,146- 95,183,240	ChIP-qPCR primer for flanking DHS nucleosome occupancy confirmation
W-chr10:95182920-	TAAGGCGAGACC	chr10:95,183,146-	ChIP-qPCR primer for

95183070 R	ACACTGAG	95,183,240	flanking DHS nucleosome occupancy confirmation
C-chr11:69388860-69389010 F	AGAAGCGGACAG TCCAGAAG	chr11:69,388,677-69,388,764	ChIP-qPCR primer for flanking DHS nucleosome occupancy confirmation
C-chr11:69388860-69389010 R	CCCTGGCTGGAA TTCATAT	chr11:69,388,677-69,388,764	ChIP-qPCR primer for flanking DHS nucleosome occupancy confirmation
W-chr11:69388860-69389010 F	CGGTAGAGCCAG CAGATAGG	chr11:69,389,098-69,389,168	ChIP-qPCR primer for flanking DHS nucleosome occupancy confirmation
W-chr11:69388860-69389010 R	AGGCTGGCTTCA AACTCAA	chr11:69,389,098-69,389,168	ChIP-qPCR primer for flanking DHS nucleosome occupancy confirmation
W-chr3:121272780-121272930 F	TGCTAACCCCTTT CCTGATG	chr3:121,273,027-121,273,121	ChIP-qPCR primer for flanking DHS nucleosome occupancy confirmation
W-chr3:121272780-121272930 R	TAGCACAGCCCA GACAGAGA	chr3:121,273,027-121,273,121	ChIP-qPCR primer for flanking DHS nucleosome occupancy confirmation
C-chr1:8087320-8087470 F	CAGGCTGGTTCA GACTCCAT	chr1:8,087,181-8,087,275	ChIP-qPCR primer for flanking DHS nucleosome occupancy confirmation
C-chr1:8087320-8087470 R	CAGTGGTAGGTG GCAGAACA	chr1:8,087,181-8,087,275	ChIP-qPCR primer for flanking DHS nucleosome occupancy confirmation
chr13:58659000-58659150 F	ATGGGTGTGGTC TTCATGCT	chr13:58,659,037-58,659,116	MNase-qPCR primer for DHS nucleosome occupancy confirmation
chr13:58659000-58659150 R	GCAGACAGGCAG AGAGTGTG	chr13:58,659,037-58,659,116	MNase-qPCR primer for DHS nucleosome occupancy confirmation
chr12:78090160-78090310 F	GGCTACAGCGTA AGGACTCG	chr12:78,090,193-78,090,286	MNase-qPCR primer for DHS nucleosome occupancy confirmation
chr12:78090160-78090310 R	TTGTTCTCGGAG GGCTTTTA	chr12:78,090,193-78,090,286	MNase-qPCR primer for DHS nucleosome occupancy confirmation
chr19:25561180-25561329 F	TGACCTTATCCG AGCCTCAC	chr19:25,561,181-25,561,257	MNase-qPCR primer for DHS nucleosome occupancy confirmation
chr19:25561180-25561329 R	CCTCCAGGTCTT TGTTACAGC	chr19:25,561,181-25,561,257	MNase-qPCR primer for DHS nucleosome occupancy confirmation
chr4:141101000-141101150 F	TTCTACCTCTAGC CTGGCTTTC	chr4:141,101,001-141,101,071	MNase-qPCR primer for DHS nucleosome occupancy confirmation
chr4:141101000-141101150 R	GGTGGGAACCAT GAGCTG	chr4:141,101,001-141,101,071	MNase-qPCR primer for DHS nucleosome occupancy confirmation
chr16:75139620-75139770 F	GCTTGTGAAGCG TCTCCTTT	chr16:75,139,677-75,139,756	MNase-qPCR primer for DHS nucleosome occupancy confirmation
chr16:75139620-75139770 R	AGCCCTGTAAGC CTCCTGAT	chr16:75,139,677-75,139,756	MNase-qPCR primer for DHS nucleosome occupancy confirmation

chr15:93432000-93432150 F	TCACGTGACATC TTTGCAAGTC	chr15:93,432,078-93,432,147	MNase-qPCR primer for DHS nucleosome occupancy confirmation
chr15:93432000-93432150 R	AACCGTCAATGG ACAAATCC	chr15:93,432,078-93,432,147	MNase-qPCR primer for DHS nucleosome occupancy confirmation
chr15:25765000-25765150 F	AGCTCCTCCCTC CTCATTGT	chr15:25,765,042-25,765,137	MNase-qPCR primer for DHS nucleosome occupancy confirmation
chr15:25765000-25765150 R	CCCACAGAGCAT CCTGACTT	chr15:25,765,042-25,765,137	MNase-qPCR primer for DHS nucleosome occupancy confirmation
chr4:53328640-53328790 F	CAACAGGGGTCT CCTTAGCA	chr4:53,328,690-53,328,773	MNase-qPCR primer for DHS nucleosome occupancy confirmation (control)
chr4:53328640-53328790 R	CTCAGGACACTG CAGGATGA	chr4:53,328,690-53,328,773	MNase-qPCR primer for DHS nucleosome occupancy confirmation (control)
chr1:51798280-51798430 F	GCTGAAGGACAG GCTTAACG	chr1:51,798,336-51,798,411	MNase-qPCR primer for DHS nucleosome occupancy confirmation (control)
chr1:51798280-51798430 R	CTTGCAAACGTTT TTCAGCA	chr1:51,798,336-51,798,411	MNase-qPCR primer for DHS nucleosome occupancy confirmation (control)
chr17:88371160-88371310 F	TACCTTTCCAGC CCCAGAGT	chr17:88,371,163-88,371,262	MNase-qPCR primer for DHS nucleosome occupancy confirmation (control)
chr17:88371160-88371310 R	CTCCCAACACTG CCTCAGTT	chr17:88,371,163-88,371,262	MNase-qPCR primer for DHS nucleosome occupancy confirmation (control)
<i>Ttc25</i> Guide -	AAACCGTGGAAA GCCTCGCAGACA C		Guide sequence to be cloned into the pX330 CRISPR Cas9 plasmid
<i>Ttc25</i> Guide +	CACCGTGTCTGC GAGGCTTTCCAC G		Guide sequence to be cloned into the pX330 CRISPR Cas9 plasmid
<i>Ttc25</i> Targ F	CTGGCTCAGCTG AATTCTGGA	chr11:100,405,951-100,407,440	Forward primer to amplify <i>Ttc25</i> 1.5kb sequence to clone into pBluescript
<i>Ttc25</i> Targ R	ggatccTAGGGGTA GTTTCGAGACCAC C	chr11:100,405,951-100,407,440	Reverse primer to amplify <i>Ttc25</i> 1.5kb sequence to clone into pBluescript
<i>Ttc25</i> Check F	CCCACAGCCATT ACTCCTGAA	chr11:100,406,404-100,406,905	Forward primer to check transfected clones for super-binder nucleosome integration

<i>Ttc25</i> Check R	CCGGTCAGACAA GTGCTGAG	chr11:100,406,404- 100,406,905	Reverse primer to check transfected clones for super-binder nucleosome integration
Superbinder nucleosome F	GCCTTAATCGGT CGTAGCAC	n/a	ChIP-qPCR primer to check histone occupancy over superbinder position
Superbinder nucleosome R	CGCGCCTAGAGG CTAGTAAG	n/a	ChIP-qPCR primer to check histone occupancy over superbinder position
WT <i>Ttc25</i> -1nuc F	TGTGCTTGGTCA AGGATCAC	chr11:100406617- 100406697	ChIP-qPCR primer to check histone occupancy over WT -1 nucleosome position
WT <i>Ttc25</i> -1nuc R	GAATTTTGGAA CGGAGTCA	chr11:100,406,617- 100,406,697	ChIP-qPCR primer to check histone occupancy over WT -1 nucleosome position
<i>Ttc25</i> flanking -1 nuc F (Primer Set D)	CCCATCACACTTT CCATTGC	chr11:100,406,510- 100,406,708	ChIP-qPCR primer to check histone occupancy flanking WT -1 nucleosome position
<i>Ttc25</i> flanking -1 nuc R (Primer Set D)	GGAAGGAGAGAG AATTTTGGAA	chr11:100,406,510- 100,406,708	ChIP-qPCR primer to check histone occupancy flanking WT -1 nucleosome position
<i>Ttc25</i> mRNA (Primer Set G)	TGTTGTTGACCA GTGGCAGT	chr11:100,415,022- 100,415,273	qPCR primer to check <i>Ttc25</i> mRNA expression levels and RNPII occupancy
<i>Ttc25</i> mRNA (Primer Set G)	TGTTGGGTACCT CCTCTTGG	chr11:100,415,022- 100,415,273	qPCR primer to check <i>Ttc25</i> mRNA expression levels and RNPII occupancy
<i>Ttc25</i> primer upstream of -1 nuc (Primer Set C)	CTCCAGGGCTGG CTAATACA	chr11:100,406,293- 100,406,363	ChIP-qPCR primer to check RNAPII occupancy upstream of <i>Ttc25</i>
<i>Ttc25</i> primer upstream of -1 nuc (Primer Set C)	TCTGTTTCAGTTC CCCCAAC	chr11:100,406,293- 100,406,363	ChIP-qPCR primer to check RNAPII occupancy upstream of <i>Ttc25</i>
<i>Ttc25</i> primer downstream of -1 nuc (Primer Set E)	TGGAATTTGCCT CCAATTC	chr11:100,406,745- 100,406,854	ChIP-qPCR primer to check RNAPII occupancy upstream of <i>Ttc25</i>
<i>Ttc25</i> primer downstream of -1 nuc (Primer Set E)	TCCAGAGTGATC GCTGTTTG	chr11:100,406,745- 100,406,854	ChIP-qPCR primer to check RNAPII occupancy upstream of <i>Ttc25</i>
<i>Ttc25</i> primer over NDR (Primer Set F)	ACGCGCTCAGCA CTTGTCT	chr11:100,406,881- 100,406,967	ChIP-qPCR primer to check RNAPII occupancy over <i>Ttc25</i> NDR
<i>Ttc25</i> primer over NDR nuc (Primer Set F)	GTTAGGCCTCCG GGTGAG	chr11:100,406,881- 100,406,967	ChIP-qPCR primer to check RNAPII occupancy over <i>Ttc25</i> NDR
DHS Guide -	CACCGAATTGGC TACTGCCAATTC		Guide sequence to be cloned into the pX330

	C		CRISPR Cas9 plasmid
DHS Guide +	AAACGGAATTGG CAGTAGCCAATT C		Guide sequence to be cloned into the pX330 CRISPR Cas9 plasmid
DHS Targ F	GGGAGTGACTTC TCCGGTTT	chr2:162754062+1627 54562	Forward primer to amplify Ttc25 1.5kb sequence to clone into pBluescript
DHS Targ R	GCTGTGGGACAC TCAACAGA	chr2:162754062+1627 54562	Reverse primer to amplify Ttc25 1.5kb sequence to clone into pBluescript
DHS Check F (Primer Set A)	GCCAAATAAAAT GGCCACAG	chr2:162754355+1627 54436	Forward primer to check transfected clones for super-binder nucleosome integration
DHS Check R (Primer set A)	GACAGTGTAGAA GAACCACTTTAA GC	chr2:162754355+1627 54436	Reverse primer to check transfected clones for super-binder nucleosome integration
DHS adjacent WT nuc F	AAGAGAAGAAGT GGCCAGGA	chr2:162754213+1627 54288	ChIP-qPCR primer to check histone occupancy flanking WT nucleosome position
DHS adjacent WT nuc R	GTGGTGTGCCCC AGATACTT	chr2:162754213+1627 54288	ChIP-qPCR primer to check histone occupancy flanking WT nucleosome position
DHS flanking WT/SB nuc (Primer Set B)	CTAGAGGTGGGT GGTTTTGG	chr2:162754165+1627 54370	ChIP-qPCR primer to check histone occupancy over DHS flanking nucleosome in either SB/SB or WT line
DHS flanking WT/SB nuc (Primer Set B)	GGCCATTTTATTT GGCTTTG	chr2:162754165+1627 54370	ChIP-qPCR primer to check histone occupancy over DHS flanking nucleosome in either SB/SB or WT line

Supplemental Table 2. Homology constructs used for creation of SB lines.

Construct	Synthetic sequence
<i>Ttc25</i> +0 SB	GCCTGCAGAATTATGTCAGGCTAGACCTTAGTTTAGACTTGCTATTAGCAAGTGTTCCATAACTATGTGACATT GAAAGCTAAACCCATCACACTTTCCATTGCATTCTCATTAACATATACCGCGTGCTAAGGCGCCTAATCGGTC GTAGCAGCTCTAGCACCCTAAACGCACGTACGCGCTGTCTACCGCGGTTAACCGCCAATAGGACGACT TACTAGCCTCTAGGCGCGTGAAGGCGTATACAAGTGATCGGTTCCAAAATTCTCTCTCCTTCCATAGGGAC CTGGAGTGCTTAAGCCTAATCCTACTTTGGAATTTTGCCTCCAATTCTCATTTTCTTGGCTTGCTTTGTCaGCG AGcgTTTCCtCGTcGCAACTGGAGGGGAGAAGCAACCTACAAGCAACACGCGATCACTCTGGAGCGCCAGCG TCCTGCAGG
<i>Ttc25</i> -60 SB	GCCTGCAGAATTATGTCAGGCTAGACCTTAGTTTAGACTTGCTATTAGCAATTAACATATACCGCGTGCTAAGG CGCCTAATCGGTCGTAGCAGCTCTAGCACCCTAAACGCACGTACGCGCTGTCTACCGCGGTTAACCG CCAATAGGACGACTTACTAGCCTTAGGCGCGTGAAGGCGTATACAAGTGATGGTCAAGGATCACGCACT AAGAAGTGACAAGAGAGAAGGCTGCCAAGCCCTCTGACTCCGGTTCCAAAATTCTCTCTCCTTCCATAGG GACCTGGAGTGCTTAAGCCTAATCCTACTTTGGAATTTTGCCTCCAATTCTCATTTTCTTGGCTTGCTTTGTCa GCGAGcgTTTCCtCGTcGCAACTGGAGGGGAGAAGCAACCTACAAGCAACACGCGATCACTCTGGAGCGCCA GCGTCTGCAGG
<i>Ttc25</i> +60 SB	GCCTGCAGAATTATGTCAGGCTAGACCTTAGTTTAGACTTGCTATTAGCAAGTGTTCCATAACTATGTGACATT GAAAGCTAAACCCATCACACTTTCCATTGCATTCTCATGCAAAATCCTCACGTCCCTGAGGGCTCTATTATTTTC CTGTTCAATTTGGCAGGTAGAACGTTAACTATACCGCGTGCTAAGGCGCCTAATCGGTCGTAGCAGCTCTA GCACCGCTTAAACGCACGTACGCGCTGTCTACCGCGGTTAACCGCCAATAGGACGACTTACTAGCCTCTAG GCGCGTGAAGGCGTATACAAGTGATTTGGAATTTTGCCTCCAATTCTCATTTTCTTGGCTTGCTTTGTCaGCG AGcgTTTCCtCGTcGCAACTGGAGGGGAGAAGCAACCTACAAGCAACACGCGATCACTCTGGAGCGCCAGCG TCCTGCAGG
<i>Ttc25</i> +180 SB	GCCTGCAGAATTATGTCAGGCTAGACCTTAGTTTAGACTTGCTATTAGCAAGTGTTCCATAACTATGTGACATT GAAAGCTAAACCCATCACACTTTCCATTGCATTCTCATGCAAAATCCTCACGTCCCTGAGGGCTCTATTATTTTC CTGTTCAATTTGGCAGGTAGAACGCGTACTTTTTCAGTTCCCTAATGTGCTTGGTCAAGGATCACGCACTAAGA AGTGACAAGAGAGAAGGCTGCCAAGCCCTGACTCCGGTTCCAAAATTCTCTCTCCTTCCATAGGGATTA ACTATACCGCGTGCTAAGGCGCCTAATCGGTCGTAGCAGCTCTAGCACCCTTAAACGCACGTACGCGCT GTCTACCGCGGTTAACCGCCAATAGGACGACTTACTAGCCTCTAGGCGCGTGAAGGCGTATACAAGTGAT TCCTGCAGG
DHS-chr2	GGAGGGGCAAGTGACGAGAAGAATGGAGACAAGACAGGCTATCTGATCAAGTCTCAAGTCTCATTATTGGGA AGGCAACTAGGGTTTATAAGCACAAATTGAGGACTGTAGCTTAGCCACAAGTGCCCTTGCAAGTGGGGGCAC TAAGCCACAAGTCCAGGCTGTGCTGAGAAGATCAGGTTGTTATCAGAGTGTTTCAAGTGTGGTGTGAGCT GCTTGCAAAAACATCGTGCTAGGAAAACAAGCAGGGTGGAAAAGTACCACCTGTAAGTAAATAGCCTGAGG TGGCTGCAGAGATGATAGCTGCTTTCTGCTAGGAATCAGCTCCCAACATTTTGCTATGTATTATAATGTAAAT TCTATAGCTGAAGGCCTATGCTGGGAGTGACTTCTCCGGTTTACAAGCTGTTGTTGTGCAAACCTGTTCTCT TGGTTTAAACTATTGGTTAAATAAAATTGGCTACTGCCAATTCCTGGAGGAACTAGAGGTGGGTGGTTTTGG GTGATGTTAACTATACCGCGTGCTAAGGCGCCTAATCGGTCGTAGCAGCTCTAGCACCCTTAAACGCAC GTACGCGCTGTCTACCGCGGTTAACCGCCAATAGGACGACTTACTAGCCTCTAGGCGCGTGAAGGCGTAT ACAAGTGATACCAGTAAGCAGTCAAAGCCAAATAAAATGGCCACAGTCTGAGTCTCATTATTTGTAAGCTAG TTAGAATAAGCTTAAAGTGTTCTTCTACACTGTCCCTCAGCAGCTGCTGTCACTTTCTGAAGGCTTACCACAT TTTTTTTTTCAGTCACATTGGATATGGGAGTAGCCACTGGCACTTACATGGATAGAGCTCAGGGAGTCTGTG AGTGTCCACAGCACAGAGGATCACCCGTGACAAAAAACCATCTGACCCAGGGGCCAGCAACGTGGAGAC TGAGAGCCCGGCTCTAAATGGATCTCCTGCAGATGTTCTGAAAGTTTTATTTTACCAGGGATATTTGTTGA GACAGGGTCTCAGTATGTAGCCAGGCTGGCTTTGAACTCACAGAGATTCCCCTGTCTCTGCCTCCCAAGT TCTGGGGGCAATTTGGAGATAAAATAAATATATATATTATCTAAAAGTGTGTATGTGTTTAGAGGTATGTA

SUPPLEMENTAL REFERENCES

Anders S, Huber W. 2010. Differential expression analysis for sequence count data.

Genome Biology, **11**: R106.

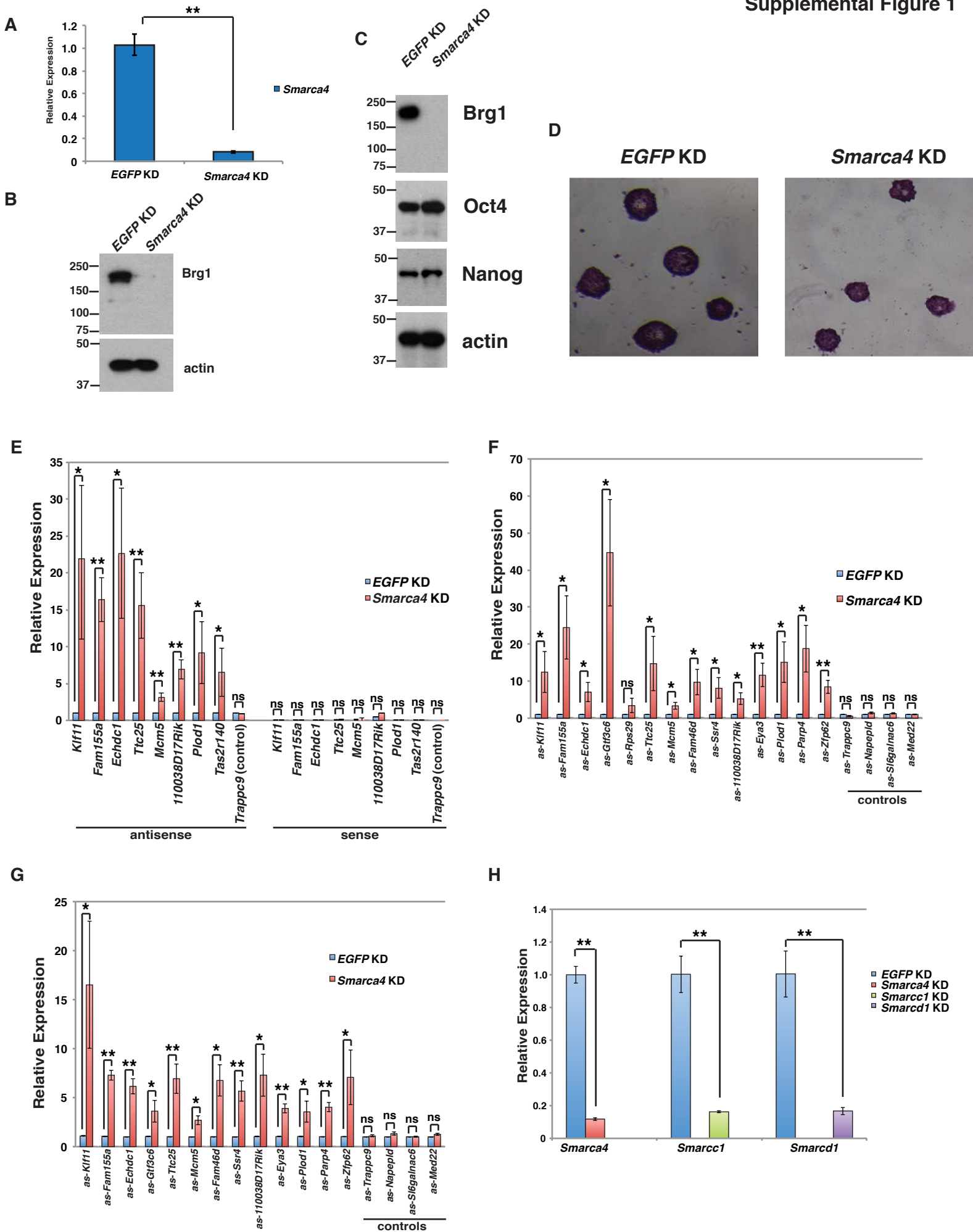
Cong L, Ran FA, Cox D, Lin S, Barretto R, Habib N, Hsu PD, Wu X, Jiang W, Marraffini

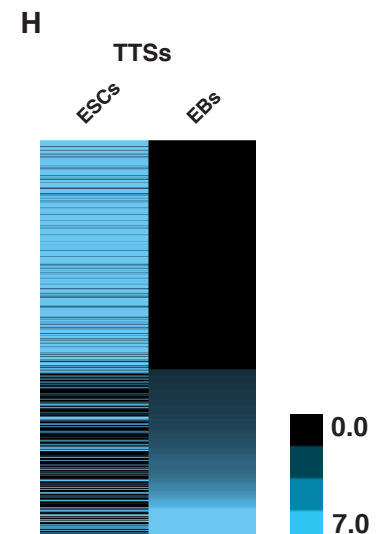
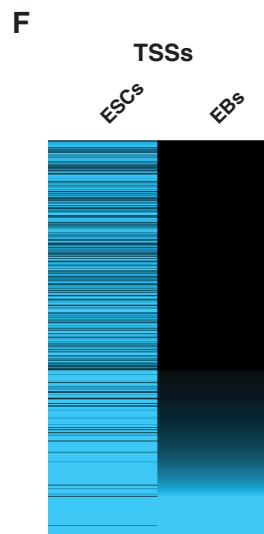
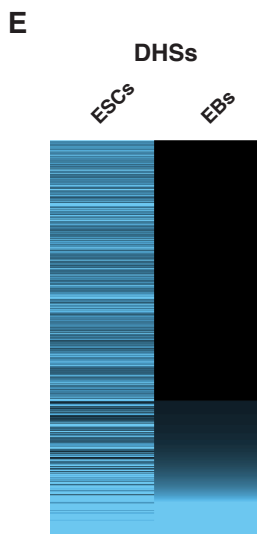
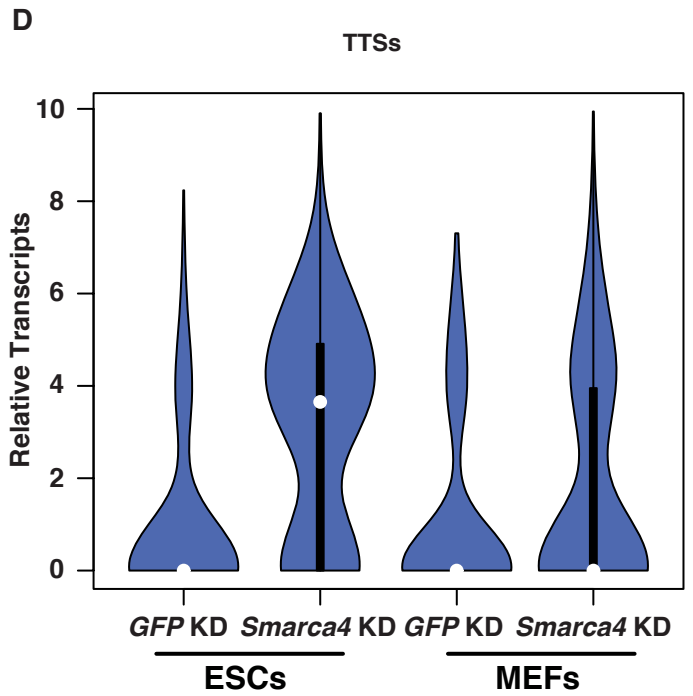
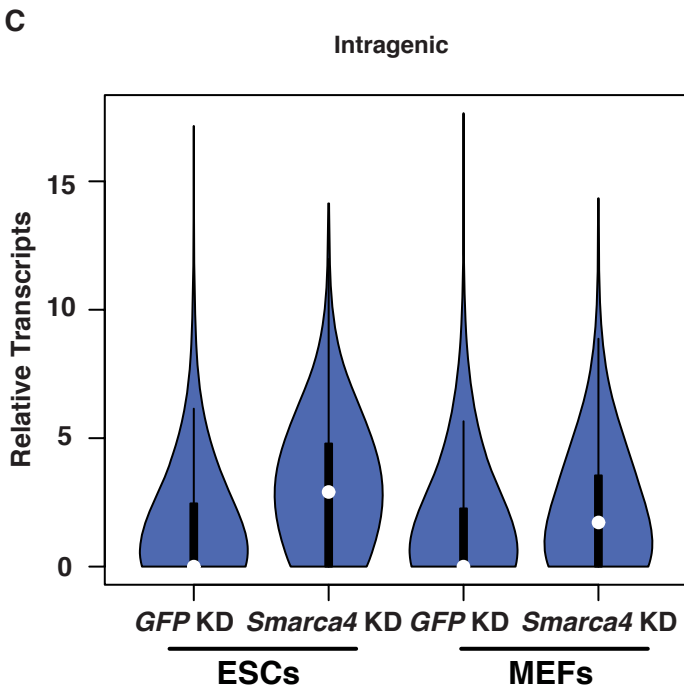
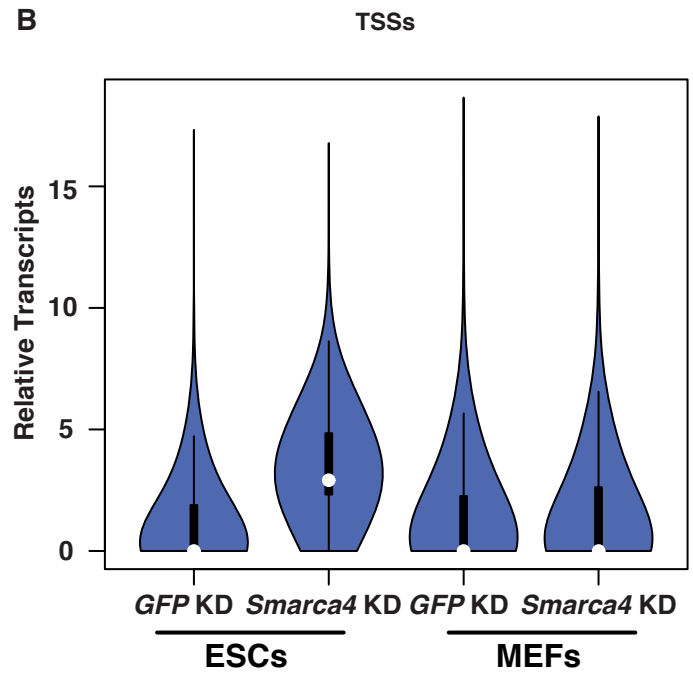
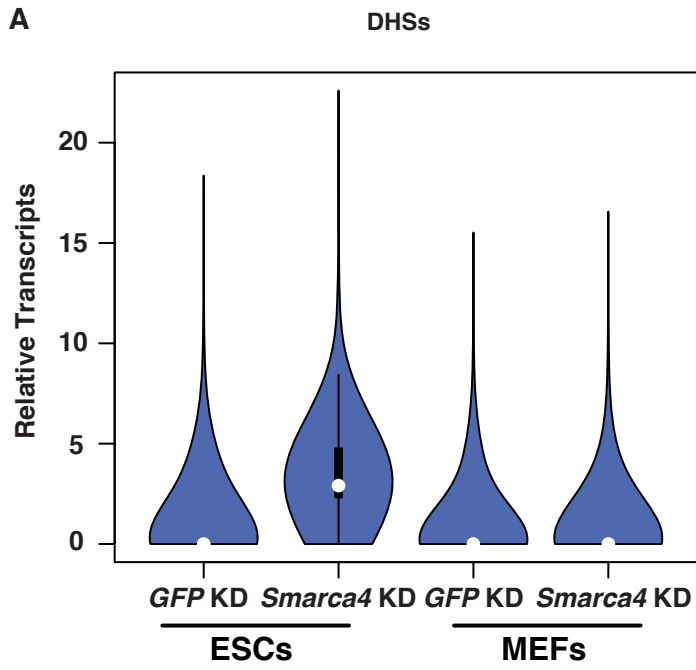
LA, et al. 2013. Multiplex Genome Engineering Using CRISPR/Cas Systems.

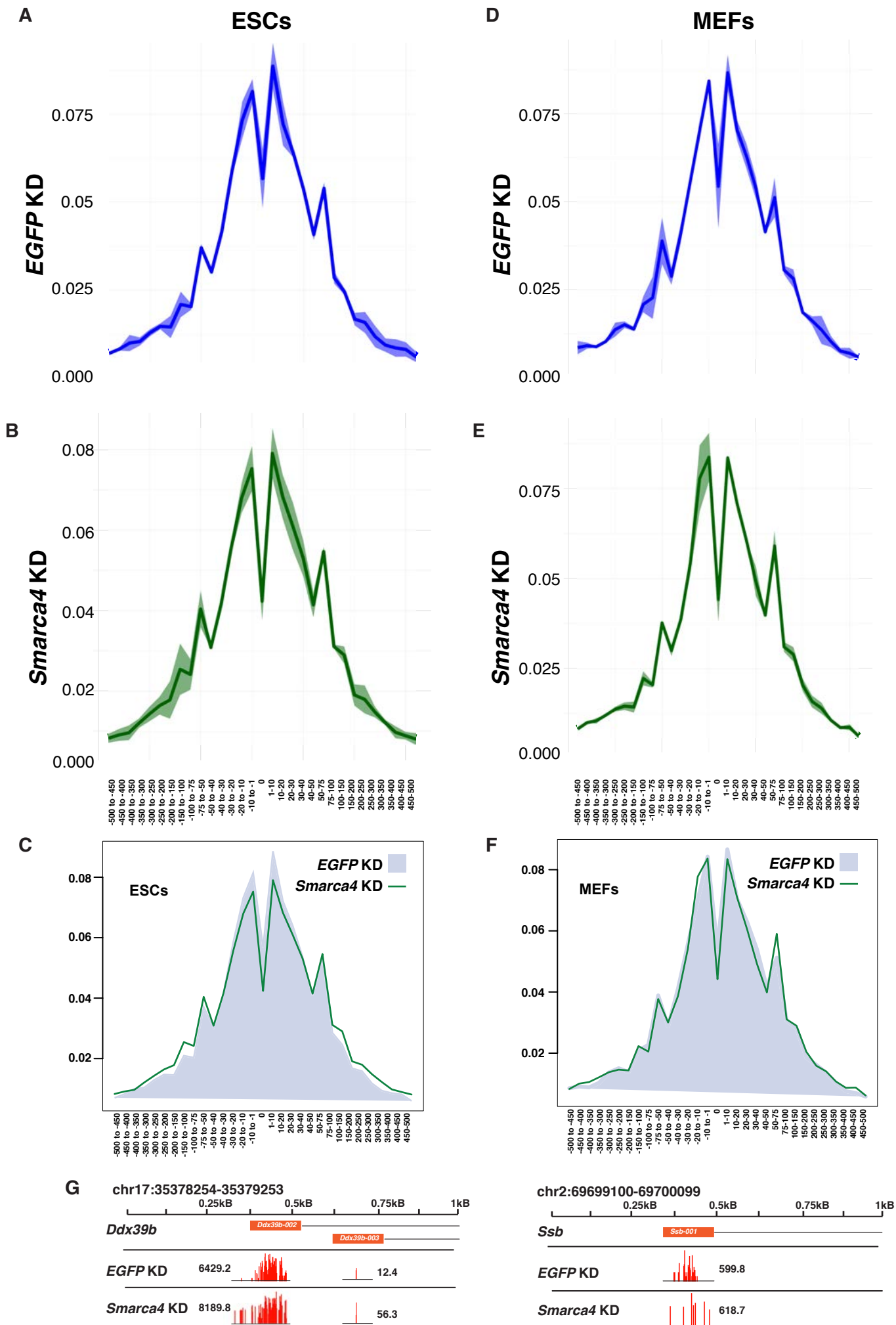
Science **339**: 819–823.

- de Hoon MJL, Imoto S, Nolan J, Miyano S. 2004. Open source clustering software. *Bioinformatics* **20**: 1453–1454.
- Gu W, Lee H-C, Chaves D, Youngman EM, Pazour GJ, Conte D Jr, Mello CC. 2012. CapSeq and CIP-TAP Identify Pol II Start Sites and Reveal Capped SmallRNAs as *C. elegans* piRNA Precursors. *Cell* **151**: 1488–1500.
- Ho L, Miller EL, Ronan JL, Ho WQ, Jothi R, Crabtree GR. 2011. esBAF facilitates pluripotency by conditioning the genome for LIF/STAT3 signalling and by regulating polycomb function. *Nature Cell Biology* **13**: 903–913.
- Kumar R, Ichibhashi Y, Kimura S, Chitwood DH, Headland LR, Peng J, Maloof JN, Sinha NR. 2012. A high-throughput method for Illumina RNA-seq library preparation. *Front Plant Science* **3**: 202
- Levin JZ, Yassour M, Adiconis X, Nusbaum C, Thompson DA, Friedman N, Gnirke A, Regev A. 2010. Comprehensive comparative analysis of strand-specific RNA sequencing methods. *Nature Methods* **7**: 709–715.
- Mituyama T, Yamada K, Hattori E, Okida H, Ono Y, Terai G, Yoshizawa A, Komori T, Asai K. 2009. The Functional RNA Database 3.0: databases to support mining and annotation of functional RNAs. *Nucleic Acids Research* **37**: D89–D92.
- Robin X, Turck N, Hainard A, Tiberti N, Lisacek F, Sanchez J, Muller M. 2011. pROC: an open-source package for R and S⁺ to analyze and compare ROC curves. *BMC Bioinformatics* **12**:77.

- Saldanha AJ. 2004. Java Treeview--extensible visualization of microarray data. *Bioinformatics* **20**: 3246–3248.
- Stein LD, Mungall C, Shu S, Caudy M, Mangone M, Day A, Nickerson E, Stajich JE, Harris TW, Arva A, et al. 2002. The generic genome browser: a building block for a model organism system database. *Genome Research* **12**: 1599–1610.
- Ye T, Krebs AR, Choukrallah MA, Keime C. 2011. seqMINER: an integrated ChIP-seq data interpretation platform. *Nucleic acids Research* **36**.
- Wang X, Bryant GO, Floer M, Spagna D, Ptashne M. 2011b. An effect of DNA sequence on nucleosome occupancy and removal. *Nature Structural & Molecular Biology* **18**: 507–509.
- Yildirim O, Li R, Hung J-H, Chen PB, Dong X, Ee L-S, Weng Z, Rando OJ, Fazio TG. 2011. Mbd3/NURD Complex Regulates Expression of 5-Hydroxymethylcytosine Marked Genes in Embryonic Stem Cells. *Cell* **147**: 1498–1510.

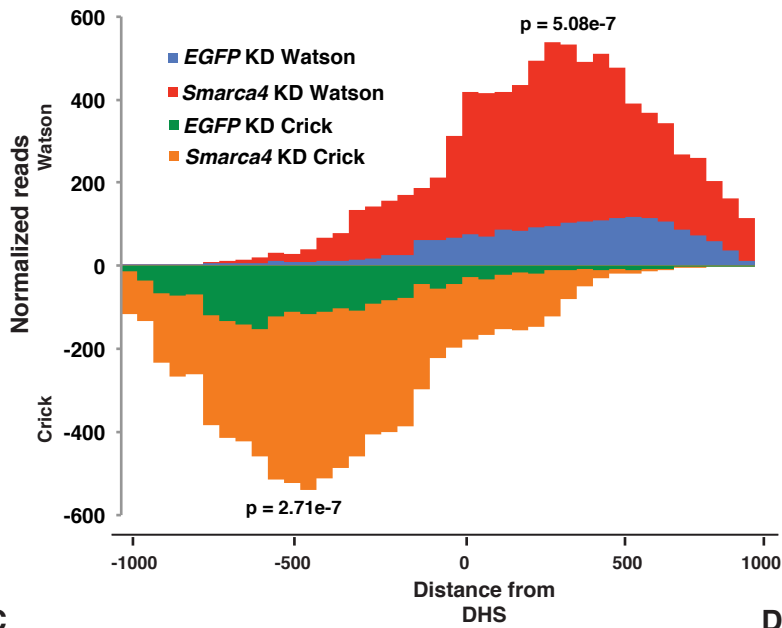






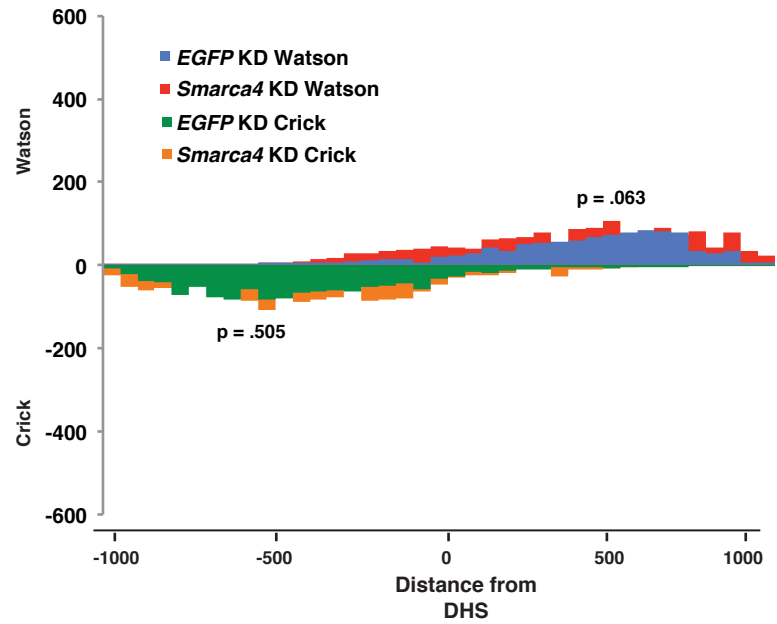
A

esBAF bound

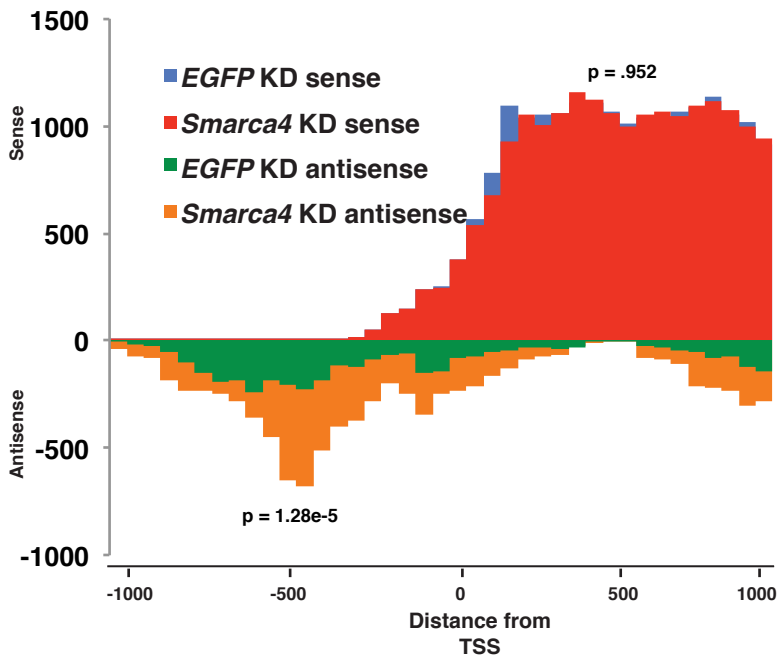


B

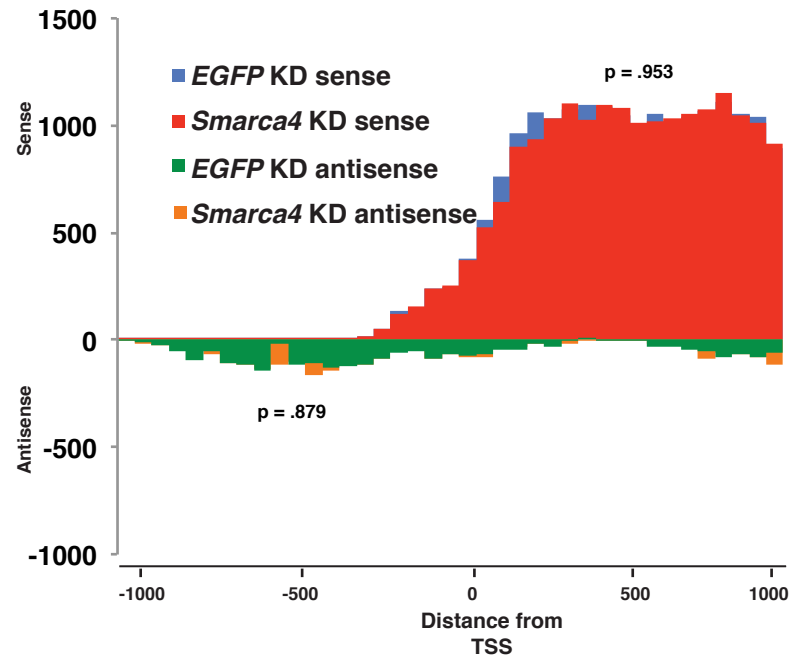
esBAF unbound



C



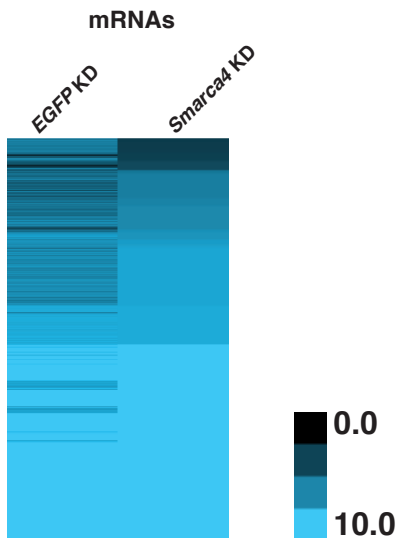
D



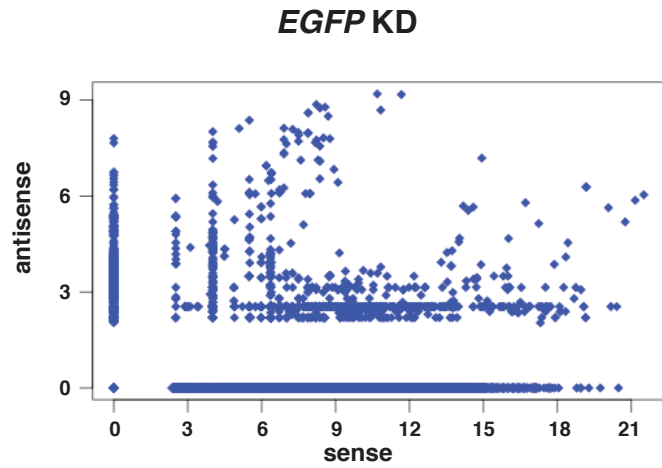
A

Fold Change	DHS		as-TSS		intragenic		as-TTS		mRNA	
	UP	DOWN	UP	DOWN	UP	DOWN	UP	DOWN	UP	DOWN
>1.5	57,237	5,271	3,631	603	2,383	238	1,031	102	1,856	2,843
>2	41,673	3,637	2,505	416	1,644	164	611	70	1,095	1,961
>3	21,482	964	1,352	125	887	89	329	38	591	1,059
>5	9,936	243	648	58	426	43	157	18	283	508

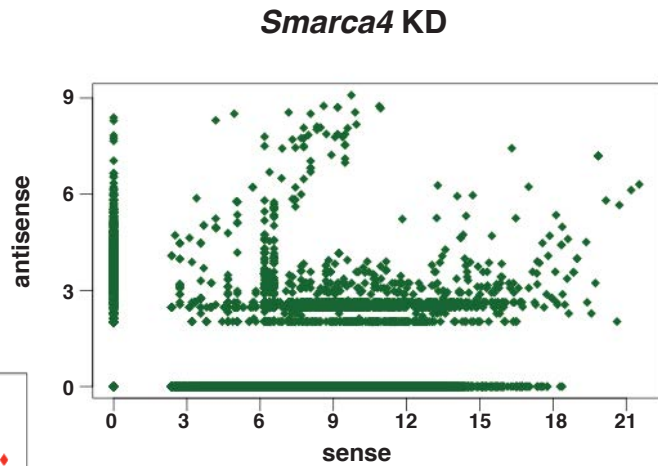
B



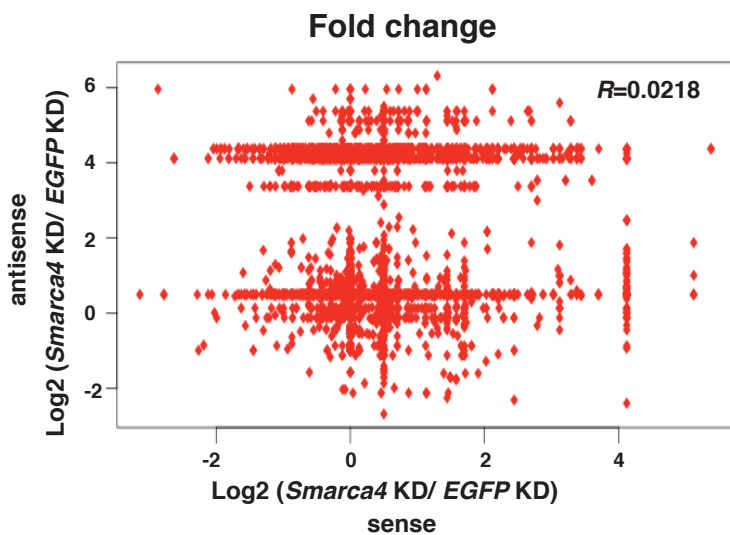
C

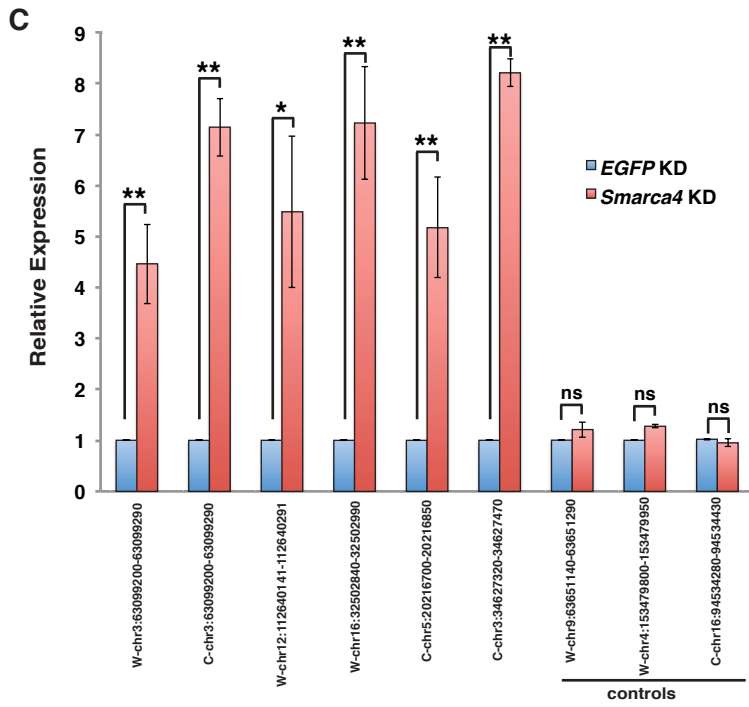
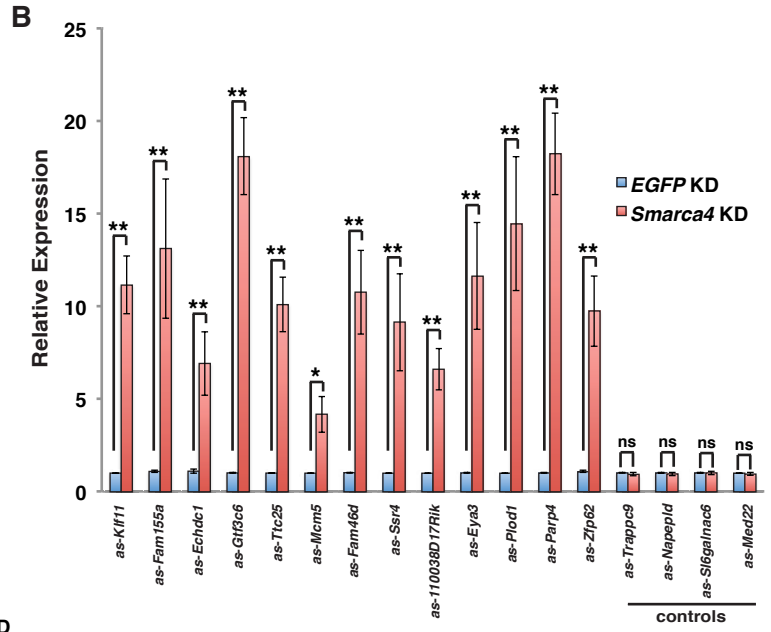
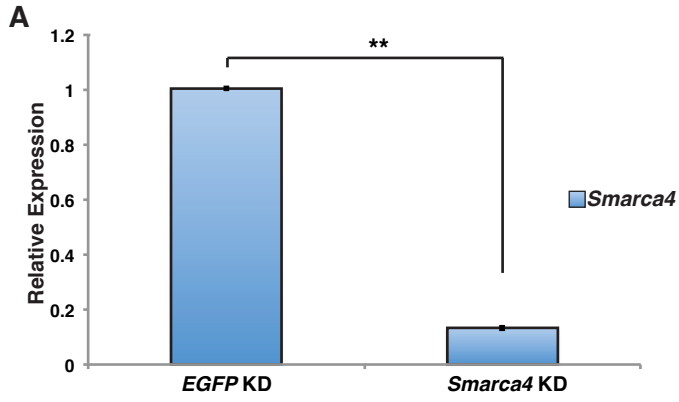


D

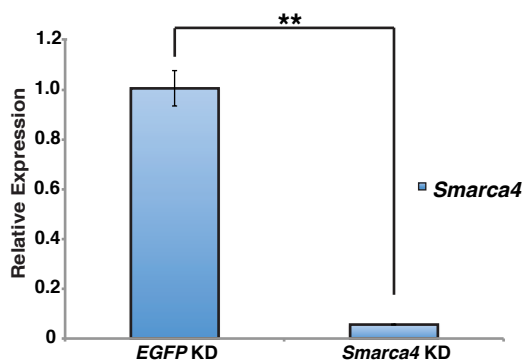


E

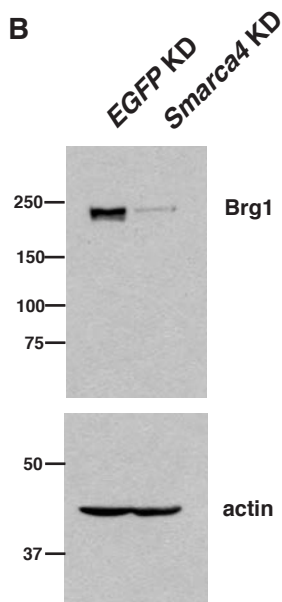




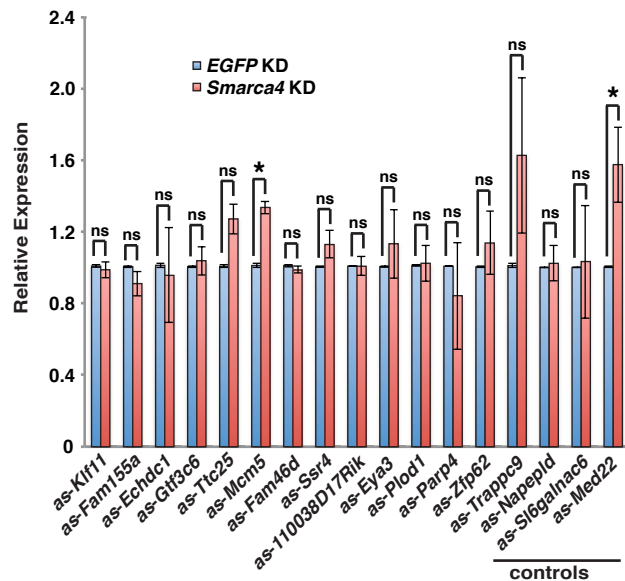
A



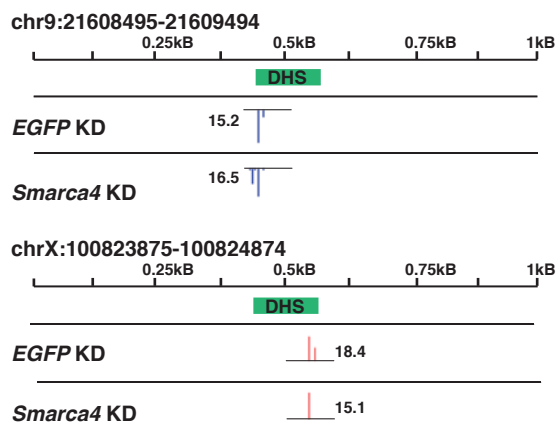
B



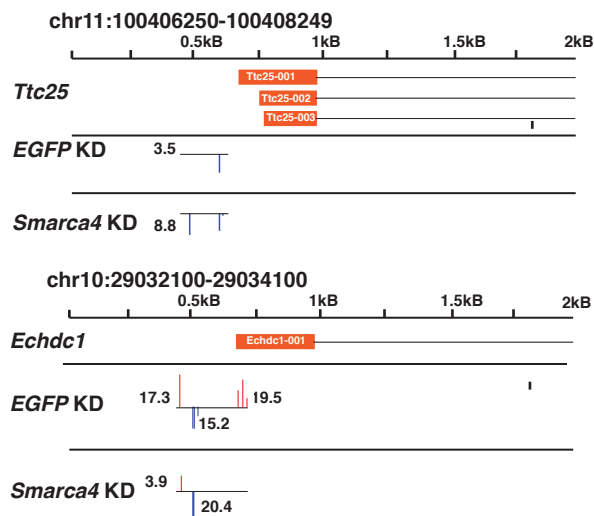
C



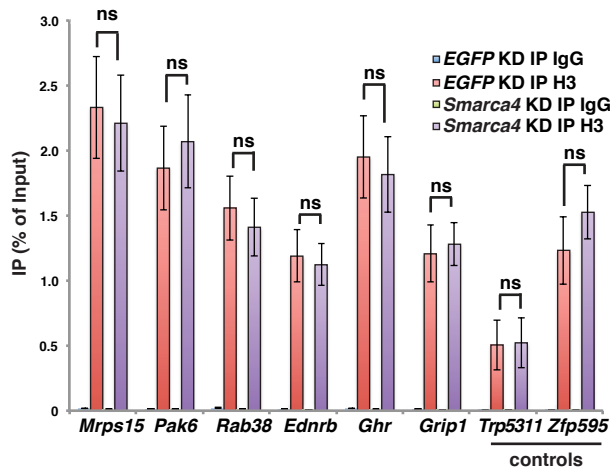
D

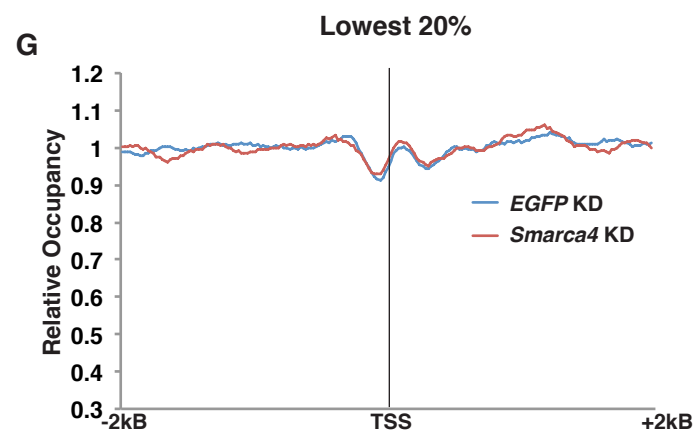
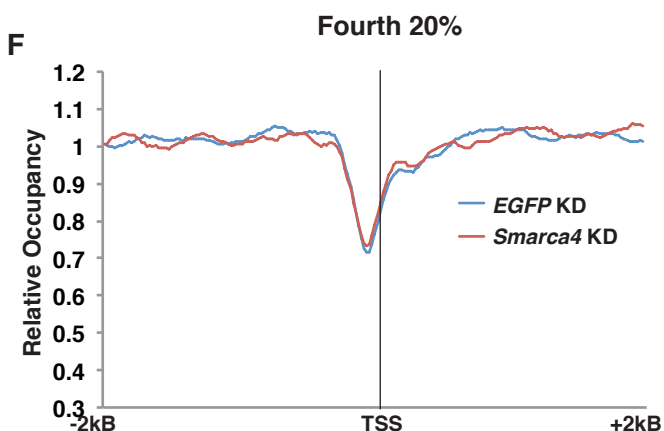
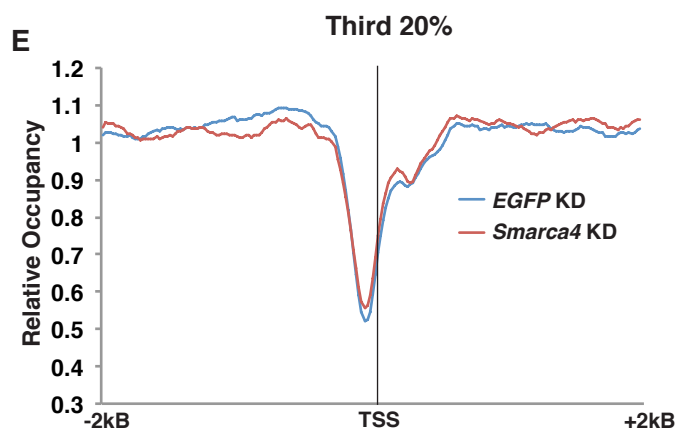
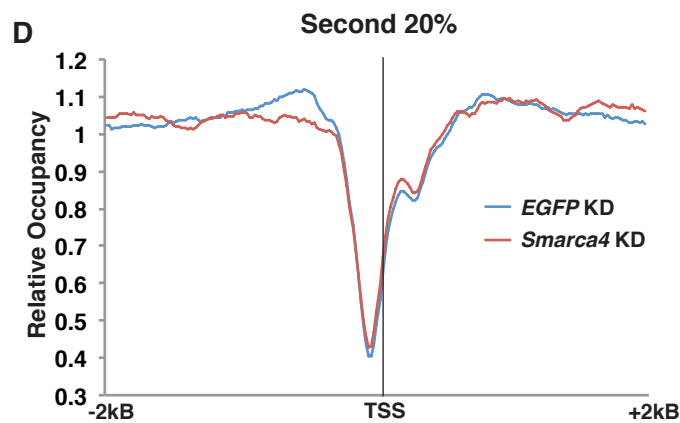
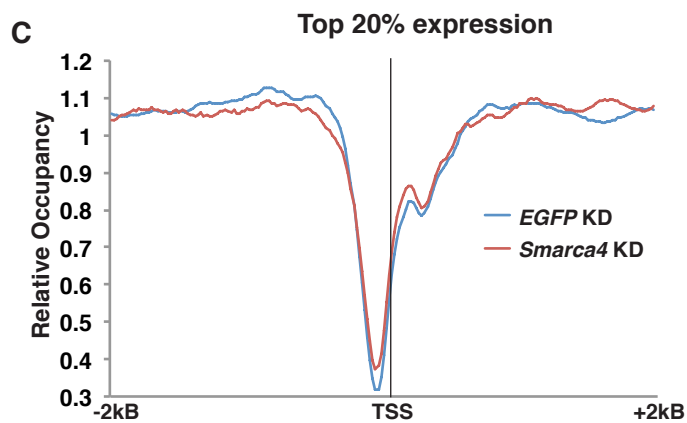
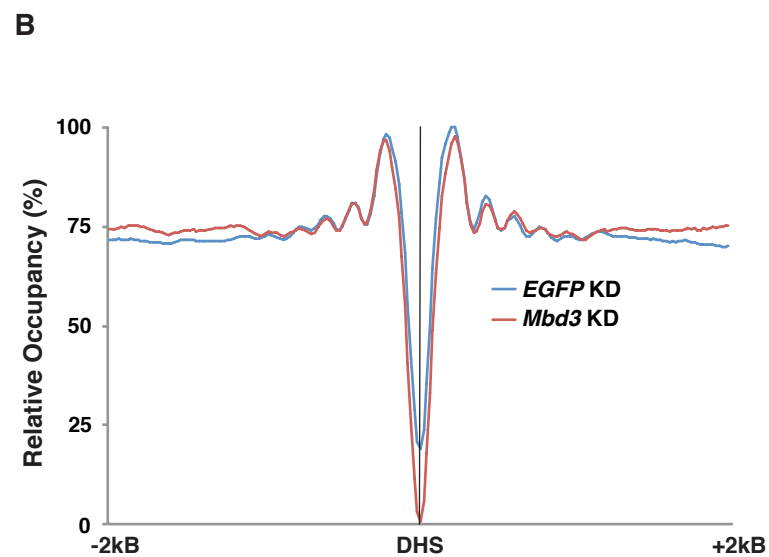
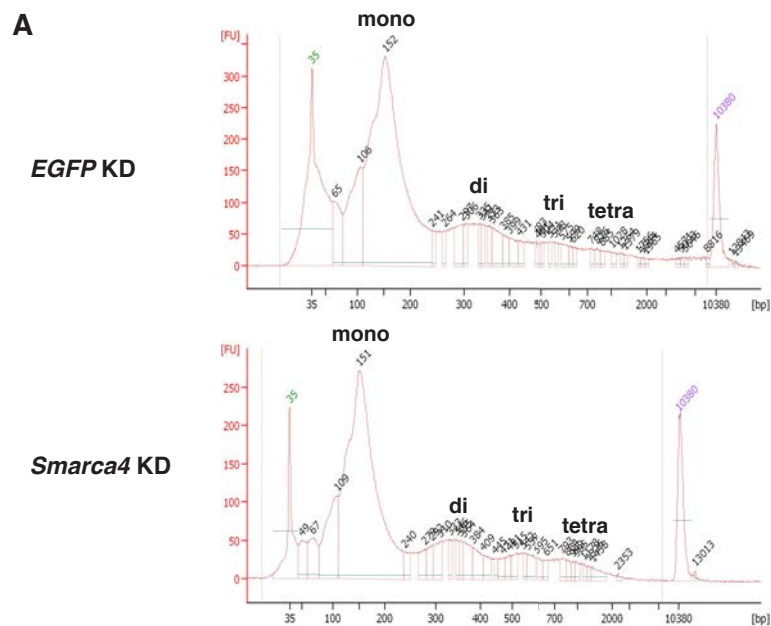


E

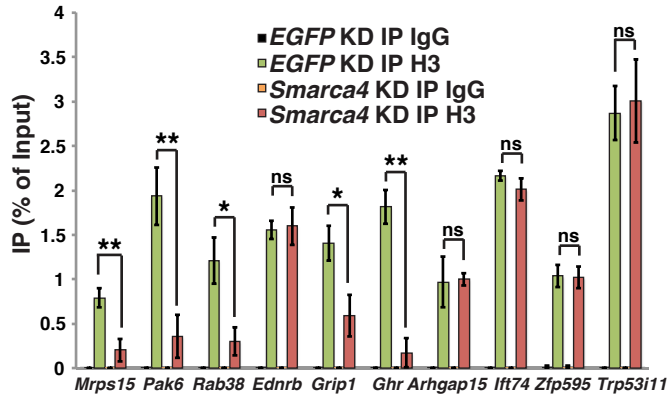


F

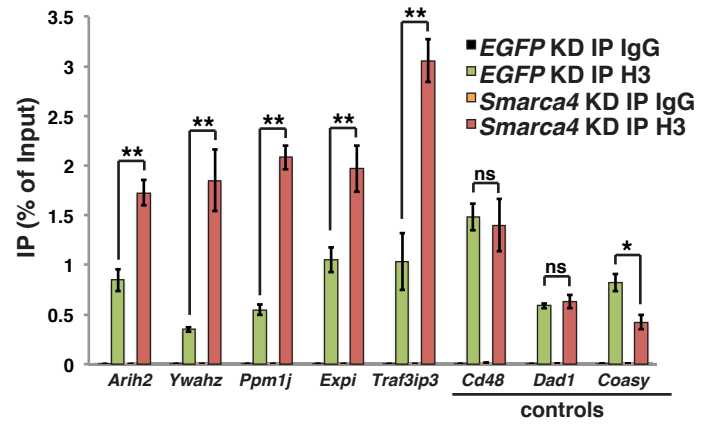




A



B



C

